VOL. 9 No. 4, p. 97-124 1947

Philips Technical Review

DEALING WITH TECHNICAL PROBLEMS
RELATING TO THE PRODUCTS, PROCESSES AND INVESTIGATIONS OF
N.V. PHILIPS' GLOEILAMPENFABRIEKEN

EDITED BY THE RESEARCH LABORATORY OF N.V. PHILIPS' GLOEILAMPENFABRIEKEN, EINDHOVEN, HOLLAND

FUNDAMENTALS FOR THE DEVELOPMENT OF THE PHILIPS AIR ENGINE

by H. de BREY, H. RINIA and F. L. van WEENEN.

621.412

The hot-air engines which were in use in the last century had a low efficiency and a large piston displacement per horse-power. Systematic investigation in the Philips Laboratories has shown that nowadays an air engine with much more favourable characteristics can be constructed. The employment of the heat-resisting steel alloys now available has made it possible to reach a mean effective pressure of 14 atmospheres (maximum pressure 50 atmospheres) and to increase the temperature of the hot chamber to 650° (centigrade). A suitable construction of heater, cooler and regenerator, based upon new insight into the compromise which must be made, in the case of these elements between heat transfer, flow resistance and dead volume, has made it possible to work with speeds of 3000 r.p.m. or more, and at the same time to ensure that the temperature of the work medium in the hot space will be only slightly lower than that of the heater, and in the cold chamber (80°) only slightly higher than that of the cooler. The high pressures and speeds have caused an improvement in the specific power by a factor of more than 100 compared with the old air engines, so that it is now of the same order as in internal combustion engines. The great temperature difference between the hot and cold spaces makes the theoretical efficiency high (like that of the Carnot process). Thanks to a radical improvement of the regenerator, increase in the mechanical efficiency, employment of a suitably constructed preheater and the natural restriction of radiation and other losses due to the small dimensions and the compact construction, the overall efficiency of the Philips air engine is also high; it is now comparable to that of internal combustion engines. Compared with the latter and with other sources of power, however, the air engine possesses a number of fundamental advantages.

Introduction

In an article in the May, 1946, number of this periodical 1) the theoretical principles of the air engine were discussed. It was then shown that the theoretical efficiency of an air engine with regenerator is equal to that of a Carnot process taking place between the same temperatures, and thus equal to the maximum possible for a prime mover within those temperature limits. If the absolute temperature of the "hot space" is T_h and that of the "cold space" T_c, the theoretical efficiency of the air engine is equal to

$$\eta = \frac{T_h - T_c}{T_h} \quad . \; . \; . \; . \; . \; . \; . \quad (1)$$

For $T_h = 920$ °K (about 650 °C) and $T_c = 350$ °K (about 80 °C), for example, $\eta = 62\%$.

This differs very much from the overall efficiencies of the previously constructed air engines, which were usually not over 3%; this value was still given for a 2 h.p. air engine in 1923 in the catalogue of a well-known firm. Moreover, the old models were very large and heavy; 800 kg was given as the weight of the above mentioned engine.

In the article already referred to 2) it was stated that in the Philips Laboratories during recent years extensive theoretical and experimental investigations of the hot-air process have been carried out, and that it has been determined that this process can be used with a much more favourable result, provided that in the construction of the engines modern knowledge about heat transfer, flow resistance etc. is applied and modern materials are used. In this way it has been found possible to build air engines which, with the same total power

---

1) The volume which takes no part in the expansion and compression and which lowers the specific power (see in I, fig. 5).

2) H. Rinia and F. K. du Pré, Air Engines, Philips Techn. Rev. 8, 129-136, May 1946.

and speed, have an efficiency just as high as ordinary internal combustion engines and can develop a still higher power than the latter per litre swept-volume (or per kilogram weight of engine).

We shall now discuss in somewhat more detail several facts which the investigations in question brought to light, as well as several new principles of construction which have been deduced therefrom and which form the fundamentals for the development of the Philips air engine. In the following, when citing the aforementioned article we shall refer to it as "I".

We shall first review in a very general manner the principle of the air engine. A certain quantity of air (or some other working medium, such as hydrogen, helium, argon or the like), which is at a high temperature, is allowed to expand in a cylinder, the hot space, where by the movement of a piston it performs mechanical work. In another cylinder, the cold space, the expanded air is cooled and compressed by the action of a piston to the original volume. It is then heated to the original high temperature. The cycle then begins anew. The compression of the air requires mechanical work; since, however, this compression takes place at low temperature and thus at low pressure, the work required is less than that which the air performs upon expansion at high temperature and thus high pressure. The engine thus produces an excess of work.

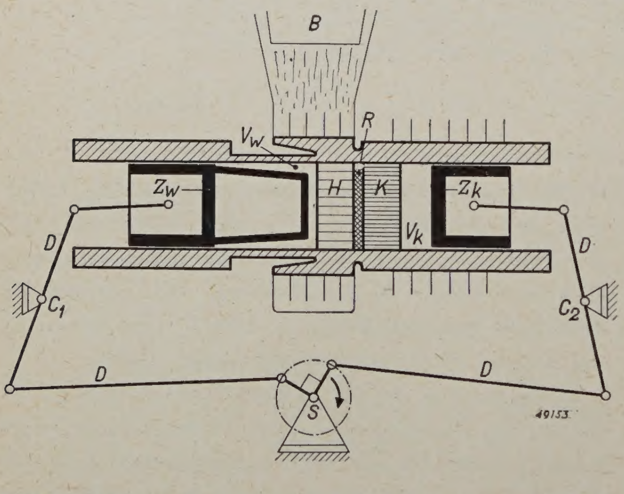

Fig. 1. Diagrammatic representation of the design of an air engine. V_w hot chamber, V_k cold chamber, with the corresponding pistons Z_w and Z_k. *B* burner, *H* heater, *R* regenerator, *K* cooler, *S* crankshaft, *D* connecting rods, C_1, C_2 fixed pivots. The pistons act on the crankshaft in such a way that the volume variations of the hot space are about 90° in phase ahead of those in the cold space.

A possible model of an air engine, very much simplified, is shown in *fig. 1*. It may be seen that the movement of the air to and fro from the hot to the cold space and *vice versa* is accomplished by two pistons moving approximately sinusoidally, whose motions are about 90° out of phase. Since the four different stages of the process: expansion, cooling, compression, heating, cannot be entirely separated, they partially overlap. In I it was shown that in spite of this the machine functions as an engine, provided the condition is satisfied that the volume changes of the hot space are advanced in phase with respect to those in the cold space. Upon the phase angle depends the power and, to a lesser extent, the efficiency. Both exhibit an only slightly pronounced maximum at a phase difference of about 90° (see I, fig. 5); while if the phase angle is chosen negative, the engine then consumes energy and acts as a refrigerator.

In fig. 1 the so-called regenerator is shown between the parts where the air is heated and where it is cooled. Its function is to store the heat which the air gives off after the expansion when passing to the cold space. When after compression the air is returned to the hot space, it again passes through the regenerator and takes up the heat stored there. As shown in I and as will be seen from what follows, the regenerator fulfils an essential function.

Let us now turn to the investigations made for the improvement of the air engine, which is the subject of this paper. These investigations, as will be clear from the statement at the beginning of this article, had a two-fold object. The first object was to improve the efficiency, the second one to increase the specific power (*i.e.* the power delivered to the main shaft divided by the swept volume). These two objects cannot actually be strictly separated: the measures taken in pursuance of them affect each other in all kinds of ways. In order to give a clear picture it is desirable first to consider the specific power.

Increase of the specific power

The power of an engine is equal to the product of the engine speed and the work per revolution. The latter, which was investigated in detail in I for the air engine, is given by the area of the p-V diagram or indicator diagram, which is represented for a certain case in *fig. 2*, curve *H*. This area is the same as that of the shaded rectangle *abcd*, whose length is equal to the piston displacement V_a, while its height is indicated as the mean effective pressure p_m.

The specific power, defined as the power divided by the piston displacement V_a, is thus equal to the product of the number of revolutions and the mean effective pressure p_m. If one desires to increase the specific power, one must try to increase both the factors above mentioned.

The mean effective pressure

In air engines in general a relatively small expansion ratio is used (see I), and the maximum pressure occurring is at most 2 to 2.5 times the minimum. The difference between the two pressures to which the mean effective pressure p_m is roughly proportional, can then only be increased by increasing the whole pressure level in the *p-V* diagram.

All the old air engines worked with a maximum pressure of only a few atmospheres, while the lowest pressure was about 1 atm. (Usually the working medium was brought for a moment into open contact with the external air at the moment of lowest pressure). Therefore, for those engines the mean effective pressure p_m was usually not higher than about 0.6 atm.

The fact that higher pressures were not used was due mainly to the lack of suitable materials for construction. The hot space of an air engine must be permanently at a high temperature. During the time when air engines were in vogue in the last century, only cast iron or bronze was available for the heated parts. The tensile strength of these metals is only small at a high temperature and especially the creep velocity at high temperature and pressure is much too high. It was therefore impossible to raise very high either the temperature (to which we shall return in connection with the efficiency) or the pressure.

It was not until around 1920 that materials became available which had a low creep velocity at high temperatures. In recent years the technology of heat-resisting metals (*i.e.* creep and oxidization-resisting) has made rapid advances. Because of this it was not only possible to get a much better construction of the air engine, but the realization of the gas turbine, the jet engine and similar engines is based upon these advances.

Thanks to the employment of modern materials it has been possible to increase the maximum pressure in the air engines developed by Philips to approximately the same level as in internal combustion engines, namely to about 50 atm. The minimum pressure is then about 22 atm., the expansion ratio 2.3, and the mean effective pressure p_m in that case is about 14 atm. This is more than twice as high as in ordinary internal combustion engines, in which, as a result of the less favourable shape of the indicator diagram, a value of p_m of the order of 6 atm. is obtained. These conditions are diagrammatically rendered in *fig. 2*. In the case of internal combustion engines somewhat higher values of p_m can also be reached, but this requires very complicated auxiliaries such as a compressor with high air yield[3]), possibly combined with an exhaust-gas turbine.

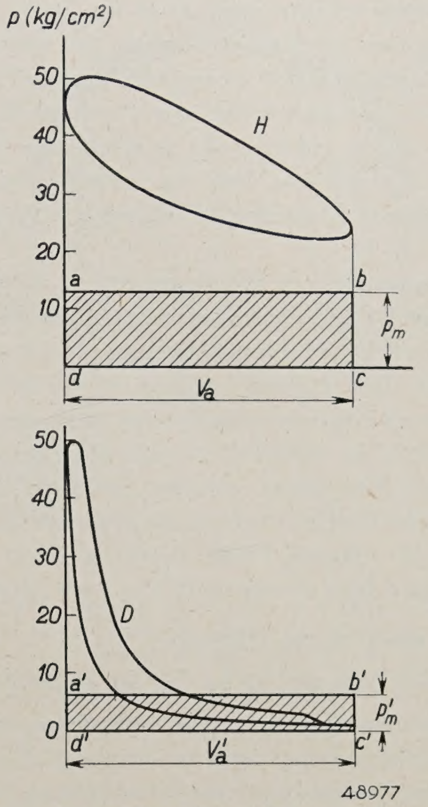

Fig. 2. Comparison of the indicator diagrams of an air engine (*H*) and a two-stroke Diesel engine (*D*). For both the maximum pressure has been chosen equal to 50 atm., while the swept volume V_a is also assumed to be equal in both cases. (Owing to the dead volume of the air engine being much larger than in the Diesel engine, the diagram for the former is actually shifted to the right with respect to the latter.) In the figure the mean effective pressures p_m are also indicated: p_m is the height of the rectangle *abcd* whose base is equal to V_a and whose area corresponds to that of the curve *H*. In the same way p_m' is the height of the rectangle *a'b'c'd'* whose area is equal to that of curve *D*. It is clear that p_m is considerably larger than p_m'.

Engine speed

The engine speed is limited mainly by two factors. In the first place the piston speed and thus the inertia forces of the moving parts increase with the engine speed. In the second place, with a higher speed the work medium must flow to and fro between the hot and cold spaces more quickly, thereby not only increasing the losses due to flow resistance, in the heater, the regenerator and the cooler, but making it more difficult to obtain the required heat transfer in these three elements. These latter questions, which are connected with the efficiency, will be discussed in more detail farther on; here we would only mention that thanks to the new construction of the three elements as developed by Philips; the problems of flow resistance and heat transfer no longer constitute any obstacle in increasing the considerably speed engine. As to the piston speeds, they become smaller the higher the pressure of the air engine is raised; as explained in the foregoing section a given power can then be obtained with a smaller swept volume. As a result it is possible to raise the speed to 3000 r.p.m. or higher, which again leads to a considerable increase in the specific power.

---

[3]) The compressor for an air engine need only be small to reach the abovementioned high minimum pressure of 22 atm. This will be explained in a subsequent article.

The magnitude of the improvement achieved in this way is made clear from a comparison with the example of the old 2 h.p. air engine already referred to, which had a swept volume of 25 litres. The same power is now attainable with an engine of only about 200 cc constructed for the same, very long life. The swept volume has thus been reduced to 1/125. The weight of the engine has also been very much reduced; in the case of a 2 h.p. engine a reduction by a factor of 50 has been attained [4]).

Improvement of the efficiency

Favourable influence of an increased specific power

In the foregoing discussion, a point was indicated where the requirements for an increase of the specific power and for the improvement of efficiency conflicted with each other where it was a question of the flow velocity of the working medium. It is remarkable, however, that in many other respects the requirements for the two objects run parallel. For example it is clear that for a given power in the case of a small engine the losses through heat radiation will be smaller than in the case of a larger engine. Moreover, in the case of a small engine these losses can more easily be reduced by heat insulation. In the Philips air engines a still higher efficiency is obtained by a very compact construction, as will be shown from a later description. The conduction losses *via* the walls of the cylinders are of course also smaller in a small engine than in a large one. This is especially true where, as in the case of the large, old engines, in order to obtain sufficient strength, the metal walls of the hot chamber had to be made very thick, a practice no longer necessary with modern steel alloys.

Another point of importance is that the earlier, clumsy air engines had to be equipped with heavy moving parts which caused large friction losses, and the mechanical efficiency, *i.e.* the ratio between the power delivered to the main shaft and the indicated power, was very low. Since the new engines can be built so much smaller, the frictional losses have been appreciably reduced. Thanks to a suitable construction in the Philips air engine they have been kept particularly low. We shall not go into this point here, since the actual construction of these engines will be dealt with in a separate article in this periodical. It can be stated however that for the latest model of the largest engines, for several hundred h.p., the mechanical efficiency amounts to more than 90%.

The temperature of the working medium in the hot and cold spaces

The losses which we have so far been discussing, all of which formerly constituted an obstacle to the attainment of a high efficiency, are in the main not specific for the air engine. Their decrease is indeed of great importance, but the most important advance in efficiency is made possible by the measures which improved the essential conditions for the hot-air process itself. In the old air engines these conditions were unfavourable in two respects: in the first place the temperature (T_h) of the working medium in the hot space was relatively low, in the cold space (T_c) relatively high; because of this, according to (1), even the theoretical efficiency was bound to be low. In the second place there was insufficient regeneration, or even no regenerator at all. We shall consider these two points separately.

One of the reasons for the relatively low temperatures formerly employed in the hot space we have already learned: the lack of materials sufficiently resistant to oxidation and at the same time free from creep. Consequently the temperature of the wall of the hot chamber — even at relatively low pressures — was limited. Another reason was the poor heat transfer to the working medium. The transfer of heat to the medium was usually allowed to take place *via* the walls of the hot space themselves. Even at the low speeds of the large old engines this was quite inadequate and as a result the temperature of the air in the hot space was usually much lower than the already relatively low wall temperature. The air temperature was seldom higher than 300 °C.

In order to improve upon this and thus, especially at high speed, to obtain a satisfactory heat transfer, a special heater was introduced, as already stated in I. This heater raises the air at the entrance to the hot space to the desired temperature, *i.e.* about 650 °C in the Philips air engine. The construction of the heater is simple in principle: a channel with a large internal wall surface, obtained for example by the introduction of a large number of internal fins of sufficient length. The air is forced to flow through the narrow slits between the fins. The inclusion of such an element in the path of the working medium, however, has its disadvantages: in the first place the flow resistance experienced by the working medium on its path between the cold and the hot space is increased; in the second place the dead volume increases. It is easy to understand that these disadvantages will be all the greater, according as one tries to improve more the heat transfer of the heater. If the channels through which the air flows into the heater are made very long and narrow, it is always possible to raise the temperature of the air at the end to the desired level; at the same time, however, there is the risk that the flow resistance will be so great at the desired high engine speed that much of the gain in efficiency will be quite lost again through the aerodynamic losses. If one tries on the other hand to make the passages for the air as wide as possible, so that the flow resistance remains sufficiently small, the dead volume again becomes large. A compromise must therefore be sought, which necessitates very careful choice of the dimensions of the heater. One of the most important tasks in the investigation carried out by Philips was to resolve the opposing differences between heat transfer, flow resistance and dead volume, which was not sufficiently understood before, and to determine the optimum conditions. It was possible to profit from the results of the numerous investigations of recent years in the field of heat transfer and theory of flow, supplemented in many respects by the results of our own research work.

---

[4]) For each type of engine the specific power can be increased and the weight limited if a shorter life (or a lower efficiency) is accepted.

Anticipating our discussion of the cooler and the regenerator, it may be stated here that the same problem arises there and a favourable construction has to be sought in a similar manner. The total aerodynamic losses in the engine with the constructions finally obtained, at a speed of 3000 r.p.m., could be limited to only about 10% of the indicated horse-power, while the heat transfer, which at this high speed has to be brought about in less than 1/100 sec., still fully satisfies the demands. Incidentally it may be noted that the decrease in the efficiency attributable to the aerodynamic losses actually amounts to considerably less than 10%, because the flow losses are converted partly into useful heat, namely in the heater and in part of the regenerator.

The construction of the heater is shown for a certain case in *fig. 3*, where the large number of channels formed by the internal fins can be seen.

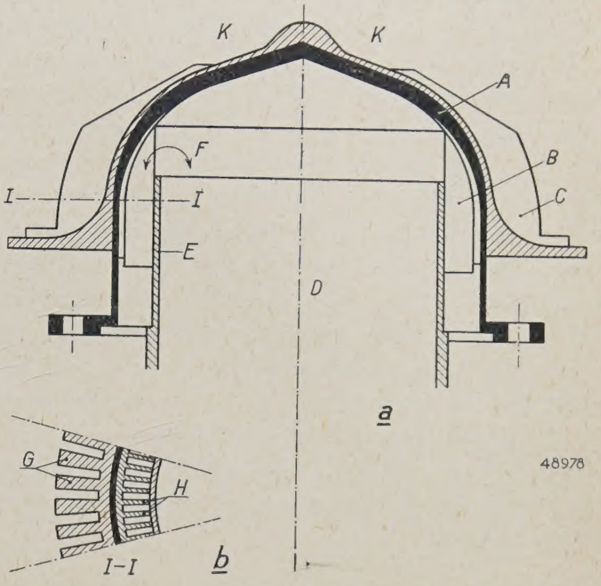

Fig. 3. Cross section of the heater of a Philips air engine; *a*) vertical cross section, *b*) part of horizontal cross section at height *I-I*. *A* bonnet of heat-resisting steel to withstand the pressure of the work medium, *B* fins of aluminium bronze for the heat exchange with the work medium (see also at *H* in the horizontal cross section), *C* fins of aluminium bronze for the heat exchange with the flame of the burner (see *G* in horizontal cross section), *D* hot space, *E* wall of the hot space. The fuel is burnt at *K*. The flame is led through the slits between the fins *G*. These and, as a result of the good heat conduction, also the fins *H*, are thus heated to the required temperature. The heat exchange with the work medium takes place in the slits between the fins *H*. The work medium can enter or leave the hot space only *via* the paths indicated by the arrow *F* (the hot space is closed at the lower side by a piston not shown here).

The outside of the heater is kept at the desired temperature by a burner. In order to ensure the best possible heat exchange also the outside is provided with fins, which are in direct contact with the flame of the burner. The internal and external fins are constructed of a good heat-conducting material, for instance aluminium bronze. This makes the temperature gradient in the fins small. The wall to which the fins are attached must be made of heat- and creep-resisting steel in order to withstand the high pressure. Since, however, this wall is thin, the slight heat conductivity of this steel has little effect.

We may briefly refer to the construction of the cold space. The mechanical requirements made of the walls here can more easily be met because of the lower temperature. As far as the heat transfer is concerned, however, this situation is analogous to that of the hot space. In order to reach and maintain as low a temperature as possible in the cold space T_c, the cooler is introduced at the entrance to the cold space. Its construction shows great similarity to that of the heater. Internally it corresponds exactly to the heater. The outside of the cooler is cooled with water or with air.

It should be pointed out that the satisfactory results obtainable with this construction of heater and cooler in practice are in fact due to the presence of the regenerator, which very much lightens the task of the other two elements. Without the regenerator the heater would have to heat the air from, for instance, 100° to 650° C each time, whereas now it has only to be heated from about 500° to 650° C. In the same way, without the regenerator the cooler would each time have to cool the expanded air from about 500° C to for instance 60° C, whereas now it is only necessary to cool from about 120° C to 60° C. This will be clearer from the more detailed discussion of the regenerator, which follows.

The regenerator

As was explained in I and again at the beginning of this article, the regenerator has to store the heat liberated as the work medium (air) passes from the hot to the cold space, and it has to give up this heat again when the movement is reversed. The importance of the function of the regenerator for the hot-air process appears most clearly when we calculate the ratio between the amount of heat q_r stored each time in the regenerator and the amount of heat q supplied per cycle by the heater to the work medium, assuming that the regenerator is ideal. With the values of T_h, T_c and the expansion ratio which are customary in the Philips air engines, the ratio $q_r/q \approx 3$ or slightly more. *The work medium thus takes up more than three times as much heat in the regenerator as in the heater.* In other words, without a regenerator the heater would have to supply about four times as much heat. The efficiency of the engine could not then be more than 1/4 of what can be attained when an ideal regenerator is present.

For the cycle actually taking place in the engine the calculation of q_r/q is rather complicated. We shall therefore calculate it only for the idealized cycle described in I of two isotherms and two isochores (two verticals of constant volume), for which it is very simple. In that case $q_r = mC_p\,(T_h - T_c)$, in which m is equal to the total mass of the air in gram molecules. Furthermore

$$q = \int_{V_2}^{V_1} p\,\mathrm{d}V = mRT_h \int_{V_2}^{V_1} \frac{\mathrm{d}V}{V} = mRT_h \ln \frac{V_1}{V_2},$$

where V_1 is the maximum and V_2 the minimum volume of the air. Now for air C_p (per gram molecule) is about $^7/_2R$. If we take $T_h = 920$ °K, $T_c = 350$ °K and $V_1/V_2 = 2$, then

$$\frac{q_r}{q} = \frac{7}{2}\,\frac{T_h - T_c}{T_h}\,\frac{1}{\ln V_1/V_2} = 3.1.$$

We thus find here a value of the same order of magnitude as that already mentioned, although it is obvious that the manner of calculation followed can only furnish a rough approximation.

From the above it follows that not only is a regenerator absolutely indispensable for good efficiency, but also that it is of the greatest importance that it should be of the best possible construction. If, say, 1% of the heat imparted to the regenerator and subsequently taken back by the work medium is lost, the performance of the heater must be increased by 3% and the efficiency drops accordingly.

It is therefore remarkable that in the earlier constructions of air engines there was often no regenerator at all. The reason for this must be sought in the above-described opposing interests between heat transfer on the one hand and the flow resistance and dead volume on the other. It was in fact quite possible to construct a regenerator with a high efficiency, but in the older constructions this was often accompanied by such a high flow resistance that it was considered preferable to dispense with regeneration.

Let us now study the requirements to be met in order to approximate an ideal regenerator as nearly as possible.

In the first place care must be taken that the heat exchange with the air takes place quickly enough. For this purpose the flow channels in the regenerator must have the correct dimensions, the above-mentioned compromise between heat transfer, flow resistance and dead volume being taken into account. In the case of the Philips air engines with high specific power the choice of this compromise is more critical than it was in the old engines of much larger volume.

In the second place a large heat capacity of the regenerator is required. With an ideal regenerator the process of storing up and giving off heat is "reversible" in every phase. In order to approximate to this it is necessary that when flowing through the regenerator the air should only differ slightly in temperature from the surroundings. The temperature distribution prevailing in the regenerator must form a certain gradual transition from the heater to the cooler. In order to maintain this temperature distribution and to obtain only slight temperature fluctuations during each revolution of the engine, the heat capacity of the regenerator must be large compared with the heat capacity of the air which flows periodically back and forth through the regenerator.

Finally the **heat conductivity** of the regenerator in the direction of flow must be slight, otherwise a continual flow of heat occurs from the heater to the cooler, which means a loss.

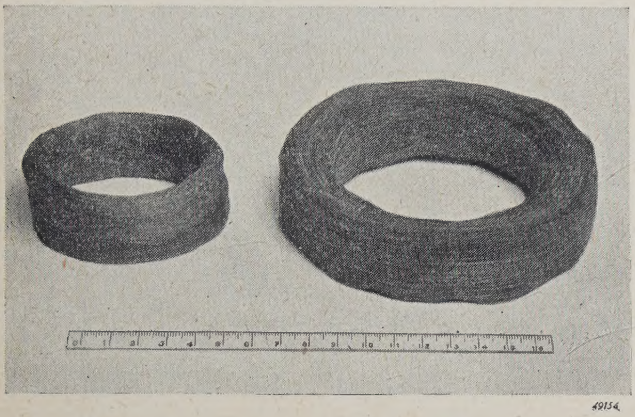

Fig. 4. Two regenerators for engines of $3^1/_2$ and 10 h.p. respectively. In the Philips air engines the air flows from the hot to the cold space through an annular shaped channel in which the regenerator is placed. (The scale is in centimeters.)

It has been found possible to construct a regenerator which comes very close to the ideal. In *fig. 4* a photograph is reproduced of two regenerators used for models of the Philips air engine of different power. These regenerators consist of a porous coil of thin metal wire. As was already stated in I, regenerator efficiencies of 95% and more are attained. It is remarkable that such a coil of metal wire is able to raise the temperature of the quantity of air flowing through it from about 100° C to about 600° C within 1/100 sec, or the reverse, and that temperature gradients of several hundred degrees per centimeter in the direction of flow can exist in it without appreciable loss of heat.

The preheater

In conclusion we will discuss a loss in efficiency which, like the losses considered at the beginning, is not specific for the air engine but which played a very large part in the case of the old engines, *viz.* the loss of heat in the exhaust gases from the burner used for heating, a loss encountered with every burner. In the case of the Philips air engine the heater has a temperature of more than 650° C. The flame and thus also the products of combustion, the exhaust gases, necessarily have a still higher temperature. If the exhaust gases are allowed to escape unused a considerable amount of heat is lost. This loss can be very much restricted by the use of a heat exchanger in which the exhaust gases give off their heat in counterflow to the air entering for the combustion.

Such a **preheater** has also been worked out for the Philips air engine. For example a certain model of it has the form of a pleated collar of heat-resisting sheet material, the exhaust gases being passed along one side of the pleats while combustion air flows along the other side. By this means a very intense heat exchange is obtained and the exhaust losses can be restricted to about 30% of the original value. *Fig. 5* shows a preheater for gaseous fuel constructed in this way and adapted especially to the design of the air engine.

Conclusion

Summarizing the results of the development sketched here, we may say that the air engine in its new form as designed in the Philips Laboratories possesses many favourable properties which until now had been considered only possible in internal

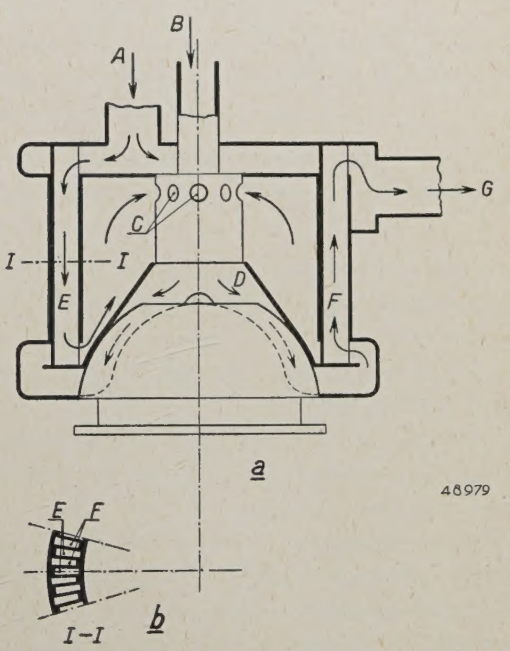

Fig. 5. Cross section through the preheater of a Philips air engine; *a*) vertical cross section, *b*) part of horizontal cross section at height *I-I*. The air for combustion enters at *A*. It follows the path of the arrows, thereby passing through the channels *E* and entering the space *D via* the openings *C*. The fuel gas — which enters through *B* — is mixed with the air in *D*, where the combustion takes place. The heater (fig. 3) along which the flame is led is indicated by dotted lines. The products of combustion are passed off *via* the channels *F* and the opening *G*. In the annular-shaped space, of which *E* and *F* represent a vertical cross section, is a pleated collar (*cf.* also the horizontal cross section). In this lie the channels *E* and *F* alternately side by side; this ensures a very good heat exchange between the air entering and the combustion products escaping.

combustion engines. It has proved possible to build compact, light, high-speed air engines of high power with an efficiency comparable to that of internal combustion engines. At the same time, however, all the fundamental advantages of the air engine over the internal combustion engine or other prime movers have been retained in the new form. We may mention here the possibility of using all kinds of fuel, low wear (since the surfaces of the cylinders do not come into contact with any corrosive gases), low consumption of lubricating oil, little noise (since there are no valves and no periodic explosions) and uniform torque thanks to the favourable shape of the indicator diagram (fig. 2). Other important advantages can only be discussed after a more detailed treatment of the design and characteristics of the new air engines. In our opinion, however, it is clear enough from the above that we are at the beginning of a very promising development.

THE IGNITION MECHANISM OF RELAY TUBES WITH DIELECTRIC IGNITER

by N. WARMOLTZ.

621.3.032.43:621.314.653

Following a short account of the most usual methods of producing an arc discharge with a mercury cathode, closer consideration is given to the capacitive method of ignition. A positive voltage of several kilovolts is applied to a conductor separated from the mercury cathode by a thin insulating wall. The action is explained on broad lines by assuming a field emission from the convex surface of the mercury against the wall of the igniter, along which the electrons move towards an auxiliary anode, this possibility being accompanied by secondary emission. The field strength at the mercury surface as deduced from measurements, however, is much too low to be able to cause field emission, so that this would seem to disprove the conception just given. A solution to the problem lies in the theory of Tonks, according to which at a certain field strength (actually reached here) the mercury surface becomes unstable and small irregularities are drawn out to sharp points, where the field strength is indeed sufficient to produce field emission. This drawing out of the mercury surface to points requires time, and this explains the measured time lag. The size of the "humps" (which must be assumed to be initially present on the mercury surface) correlating the measured time lag with the "drawing out" time calculated by Tonks agrees with the calculated thermal irregularity of a mercury surface. In conclusion several applications are discussed of relay tubes with dielectric ignition.

Survey of the methods of ignition of a mercury arc

Discharge tubes with a pool of mercury as cathode have been used for many years, for instance in the form of mercury-cathode rectifiers. Here the arc discharge emanates from a small part of the mercury surface, the so-called cathode spot. This intensely luminous spot, in which the current density is very high, moves around over the mercury in no defined course. Generally, special means have to be employed to bring it about. Formerly, and not infrequently still now, this ignition was initiated by interrupting the contact between the mercury cathode and a starting electrode forming part of an electric circuit.

In the course of time various constructions have been invented, of which we shall mention only a few here, namely those based upon:

a) the tipping of the whole discharge vessel, thereby breaking a mercury bridge between the starting electrode and the mercury cathode;

b) the raising of the starting electrode out of the pool of mercury (by means of an external magnetic coil);

c) the flowing back of mercury previously raised some way or other until it had made contact with the starting electrode.

Since a cathode spot can only exist as long as the current is above a certain limit (of the order of 5 amp.), mercury cathode rectifiers are usually provided with one or more auxiliary anodes whose current maintains the cathode spot even when the current of the main anode(s) falls below the critical limit. This makes it unnecessary, in the latter event, for the ignition mechanism to come into action again. A permanent auxiliary discharge, however, has its disadvantages, such as:

1) the increased risk of arc-back (passage of current in the wrong direction) owing to the continual presence of ionization, and

2) the not inconsiderable energy dissipation in the auxiliary discharge, at least in rectifiers for low power.

In the last decades great interest has arisen in discharge tubes in which the passage of current can be made to begin at precisely determined moments (relay tubes). Such tubes are practically inertia-free switches. In principle the above mentioned rectifiers with mercury cathode can be used if they are provided with control grids, but then, in addition to the objection just mentioned in connection with the permanent auxiliary discharge, there arises a third drawback, in that the ions from that discharge create the possibility of discharges (in the right direction) at moments when they are undesired.

For these reasons it was desirable not to have a permanent cathode spot but to seek means of causing the spot to arise only when it is needed. This we call controlled ignition. It can be used, for instance, for starting a relay tube at each cycle of the A.C. voltage used. In principle control grids thus become superfluous, because their function of opening the passage for current at certain moments is performed by the ignition arrangement.

Controlled ignition

The above-mentioned methods of ignition are unsuitable for controlled ignition because of the mechanical inertia and the waves present on the surface of the mercury. However, two other methods have been developed which are free of these drawbacks. In the older of these an external ignition band is applied, which method was made publicly known in 1901 by Cooper Hewitt. [1]) A modified version of this dielectric ignition will be discussed in this article. The other method, which we shall not discuss, was discovered in 1933 by Slepian and Ludwig [2]); it makes use of a semiconductor partly immersed in the cathode mercury.

Fig. 1a is a diagram showing the principle of a valve with the original ignition band. A conducting band is laid round the glass envelope of the discharge valve at the level of the mercury meniscus. When applying to this band a sufficiently high voltage impulse, positive with respect to the mercury cathode, a spark occurs near the place where the mercury touches the glass wall, thereby forming a cathode spot, after which the discharge is taken over by the anode. For smooth ignition, especially where the anode voltage is low, it is advisable to use an auxiliary anode connected to a point of high voltage, for instance the ignition band itself.

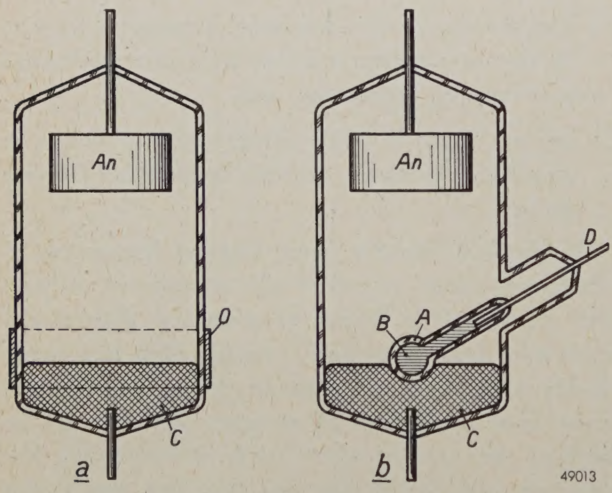

Fig. 1. *a*) The ignition band (*O*) of Cooper Hewitt is a metal band laid around the outside of the glass discharge vessel at the height of the meniscus of the mercury cathode *C*. A voltage impulse of about 10 kV applied to *O* and positive with respect to *C* causes a cathode spot on the mercury near the glass wall, after which a discharge to the anode *An* develops which further maintains the discharge.

b) Sketch of the internal dielectric igniter. *A* insulating wall, *B* conductor, *C* mercury cathode, *D* voltage lead to the starter.

Later on, several investigators recommended the form of an internal dielectric igniter, or starter, as illustrated in fig. 1*b*. An insulating tube, for instance of quartz, filled with a conductor is partially immersed in the cathode mercury. A positive voltage impulse of sufficient strength applied to the internal conductor causes the formation of a cathode spot on the outside of the starter. Here, too, an auxiliary anode may be desirable; the non-insulated part of the supply lead (fig. 1*b*) may serve as such.

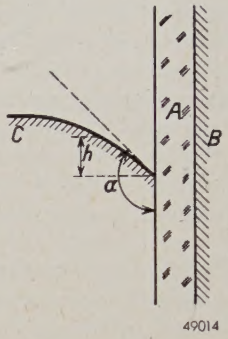

Fig. 2. Shape of the mercury meniscus at the igniter. The letters *A*, *B* and *C* have the same meaning as in fig. 1*b*. α is the so-called boundary angle, which varies for different substances and for the combination mercury-quartz amounts to about 135°. The position of a point on the convex mercury surface is determined by the height *h* above the boundary line between the mercury and the wall of the igniter.

The spark from which the cathode spot originates is formed in the gap between the convex mercury meniscus and the insulating wall of the starter. *Fig. 2* is an enlarged diagram of this gap. We shall revert presently to the phenomena taking place in this gap.

Sketch of the process of ignition

In broad lines one might picture the ignition process as follows: the positive voltage on the conductor in the starter sets up in the gap mentioned above an electric field which, when it is strong enough, causes a field emission (also called cold emission) of electrons from the mercury. This current of electrons flows to the wall of the starter, which is at a positive potential, and is conducted along it (probably due to the occurrence of secondary emission) to higher parts of the wall at a higher positive potential until it reaches the auxiliary anode. Along their path the electrons ionize mercury atoms, thus converting the electronic discharge into an arc discharge. The formation of an arc from a glow discharge [3]) must be considered out of the question; the pressure prevailing under these conditions (saturated mercury vapour at about room temperature) is too low, the distance between the electrodes is too small and the voltages (less than 10 kV) are too low for the occurrence of a glow discharge.

---

[1]) U.S. patent 682 691.

[2]) Trans. A.I.E.E. 52, 693, 1933.

[3]) See for example M. J. Druyvesteyn and J. G. Mulder, Philips Techn. Rev. 2, 122, 1937.

This picture of the mechanism may be true in the main if the two following questions can be answered in the affirmative:

1) In an arrangement like the one used but in a vacuum (in order to avoid the complications of the gas discharge), can a field emission cause a current to flow to an auxiliary anode?
2) In the customary capacitive starters, is field emission in mercury possible with the field strengths occurring there?

We shall now describe some experiments [4]) from which it is to be concluded that the answer to the first question is, indeed, in the affirmative. As to the second question, the answer to that seems at first sight to be in the negative, but given a certain mechanism preceding the field emission this difficulty is solved and at the same time the ignition lag, which will be discussed below, is explained.

Verification of the assumed process of ignition

Electron emission in a vacuum

Fig. 3 is a sketch of the valve with which we demonstrated the occurrence of field emission. The invaginated part *A* of the glass envelope corresponds functionally to the starter wall *A* in fig. 1*b*. The internal conductor consists of a cable of stranded copper wire inserted loosely in the tube *A*. Since in this experiment we wish to avoid the presence of gas, there must be no mercury in the tube. The cathode therefore consists of a layer of graphite deposited on the inner wall and brought into contact with a helical spring. An anode is connected to the internal conductor. The tube is evacuated to a pressure of 10^{-5} mm Hg or less. When a D.C. voltage of the order of some thousands of volts is applied between the graphite and the internal conductor (the latter positive), a current can be detected across the anode. This current continues when the conductor is taken out of the inner tube *A*; without the conductor having been placed in the inner tube, however, there can be no current.

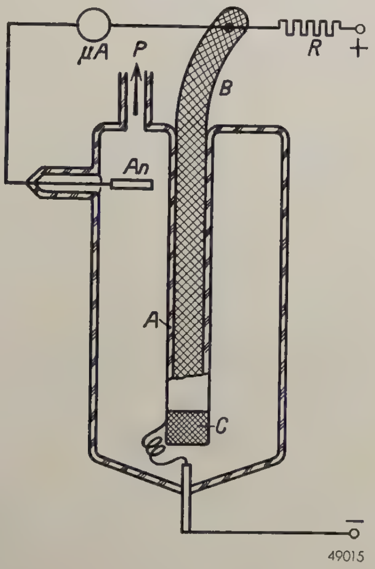

Fig. 3. Experiment for the demonstration of field emission in vacuum. The invaginated tube *A* of a glass envelope is covered at the end with a layer of graphite *C* making contact with a helical spring. The valve is exhausted through the pump tube *P*. A cable *B* of stranded copper wire is inserted in the inner tube *A* and connected *via* a galvanometer with the anode *An* and *via* a resistance *R* of 100 megohms with the positive terminal of a source of D.C. voltage. The negative terminal is connected to *C*. At a voltage of several kilovolts a current is measured across *An* which continues to flow when the conductor *B* is taken out of the tube *A*. This current, however, begins to flow only when *B* is in *A*.

This is explained in the following way: when the conductor is inserted in the inner tube and comes to lie immediately opposite the rough graphite surface, then at that surface there is a field strength high enough to cause field emission, the electrons emitted move towards the vacuum side of the glass inner tube, and would give this a negative charge and thus screen off the field if there were no secondary emission to keep the wall surface at a high positive potential. This process may be repeated one or more times until finally the secondary electrons reach the anode.

The fact that the current still continues to flow after the conductor is removed supports the assumption of secondary emission. How, otherwise, could the graphite continue to emit electrons if the wall *A* (fig. 3) were not kept at a high potential. This is only possible where there is secondary emission. But the internal conductor is needed to start the discharge, because otherwise the cathode cannot be given the field strength necessary for the field emission.

Let us now turn to the second question: whether with the usual starters the field strengths are sufficient to cause field emission.

The field strength at the cathode

The experiment just described demonstrates in principle the possibility of the occurrence of field emission, perhaps followed by secondary emission from the starter wall. There are, however, considerable differences between the situation existing in this experiment and that of a starter immersed in mercury. As to the field strength at the cathode surface in the latter case, the experiment of fig. 3 cannot teach us much. In the first place, in the situation given in fig. 3 there was no gap such as occurs where there is a mercury meniscus (fig. 2), and in the second place the graphite layer was rough, whereas the mercury, at least apparently, is smooth. It is known that higher field strengths occur locally on a rough surface than on a smooth one.

---

[4]) See for a more detailed description of these experiments (and others in the same field) N. Warmoltz, On the mechanism of dielectric igniter and of the semi-conductive igniter in mercury-vapour rectifiers, thesis, Delft 1946.

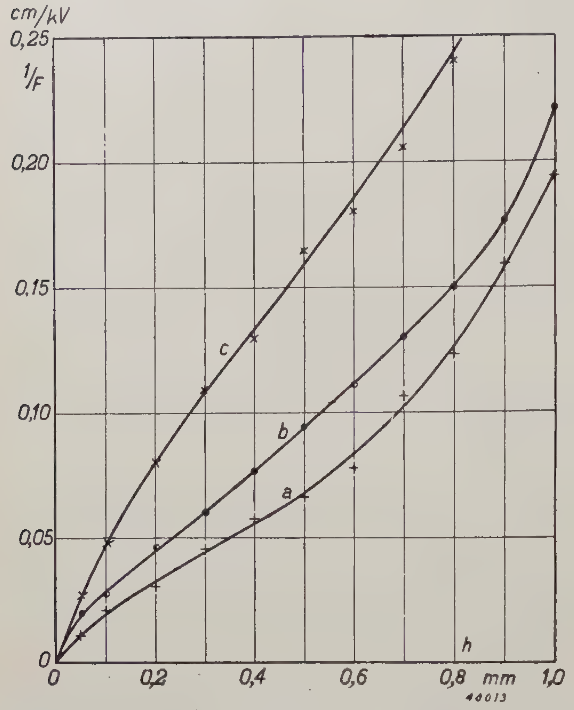

Fig. 4. Field strength F at the mercury surface at a voltage of 1 kV on the igniter. $1/F$ (F in kV/cm) is plotted as a function of the height h above the boundary between the mercury and the starter wall. Curves a, b and c are for walls with $\varepsilon = 4.4$ respectively 0.35, 1.0 and 3.0 mm thick. They are derived from measurements described in the article cited in footnote [5]).

The field strength on the supposedly smooth mercury surface can be deduced from the distribution of potential in the space between the meniscus and the starter. Measurements carried out on models in an electrolytic tank have already been described in this journal [5]). From these measurements the field strength F at the mercury surface has been derived as a function of the height h above the boundary line between the mercury and the starter wall, and for a given potential difference (1 kV) between the mercury and the interior of the starter. The result depends also upon the thickness and the dielectric constant ε of the starter wall. Curves for quartz ($\varepsilon = 4.4$) in thicknesses of 0.35 mm, 1.0 mm and 3.0 mm are given in *fig. 4*, where $1/F$ (for easier extrapolation to small values of h) is plotted as a function of h.

The next step is to find where the spark occurs. This place (fixed by the height h above the boundary line) is determined directly with the aid of a magnifying glass. We used an ignition band as shown in fig. 1a. This band consisted of a layer of silver so thin as to be transparent, so that the height at which the spark occurred could easily be seen. With a given starter this height was found to depend upon the voltage V applied to the starter. *Fig. 5* shows this relation between h and V for a given case (wall of 0.35 mm quartz). The higher the voltage V, the deeper the spark occurs in the gap.

The field strength on the mercury at the place where the spark occurs is found from a combination of figs. 4 and 5. From fig. 5 we find for a wall of 0.35 mm quartz and for values of V from 3.00 to 6.55 kV, the values of h given in *table I*, to which correspond, according to fig. 4, the values of the field strength F given in the last line of the table.

Can field emission be expected with these field strengths? Haefer has determined the field strength necessary for field emission in the case of tungsten [6]). His measurements are in agreement with the theoretical deductions. He found, for example, that with a field strength of 3×10^4 kV/cm there is a current density of 45 amp/cm^2, but that with a field strength three times as small it is only 3×10^{-16} amp/cm^2. The same applies to mercury, where the work function (4.4 V) is practically the same as for

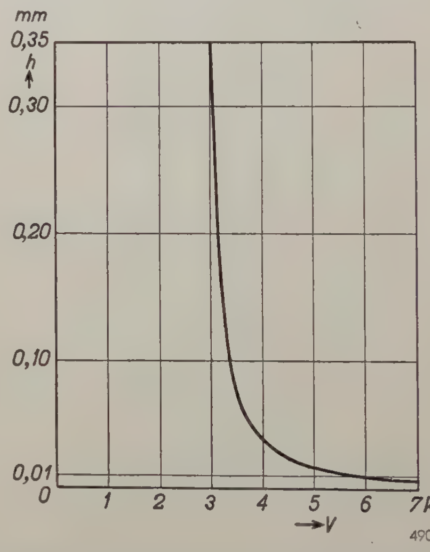

Fig. 5. Measured height h at which sparking takes place on the mercury cathode (in the case of a given igniter) with a function of the voltage V applied between the igniter (+) and the mercury cathode (—).

Table I. Height h at which the spark occurs and field strength F on the mercury for several values of the voltage V on a starter with a wall of 0.35 mm quartz.

V (in kV) =	3.00	3.15	3.55	4.50	6.55
h (in mm) =	0.35	0.21	0.065	0.025	0.008
F (in kV/cm) =	50	94.5	255	750	2500

---

[5]) N. Warmoltz, Potential distribution at the igniter of a relay valve with mercury cathode. Philips Techn. Rev. **8**, 346, 1946.

[6]) Z. Phys. **116**, 604, 1940.

tungsten. The field strength of 10^2—10^3 kV/cm cannot, therefore, cause any appreciable field emission. We shall presently see how this difficulty can be satisfactorily solved.

The time lag of the ignition

If the ignition does indeed take place according to the process sketched above, one would not, *a priori*, expect any larger time lag (the time elapsing between the discharge and the moment when the ignition voltage is applied) than the time taken by the current of electrons to pass over into an arc (*i.e.* the time for building up the gas discharge). Sparking measurements taken by various investigators in an evacuated tube have shown that this building-up time is very short, of the order of 10^{-7} sec. Nevertheless, oscillograms of the voltage on the starter show that much longer time lags occur, as has been demonstrated with the apparatus of *fig. 6*; this is explained further in the text underneath the diagram.

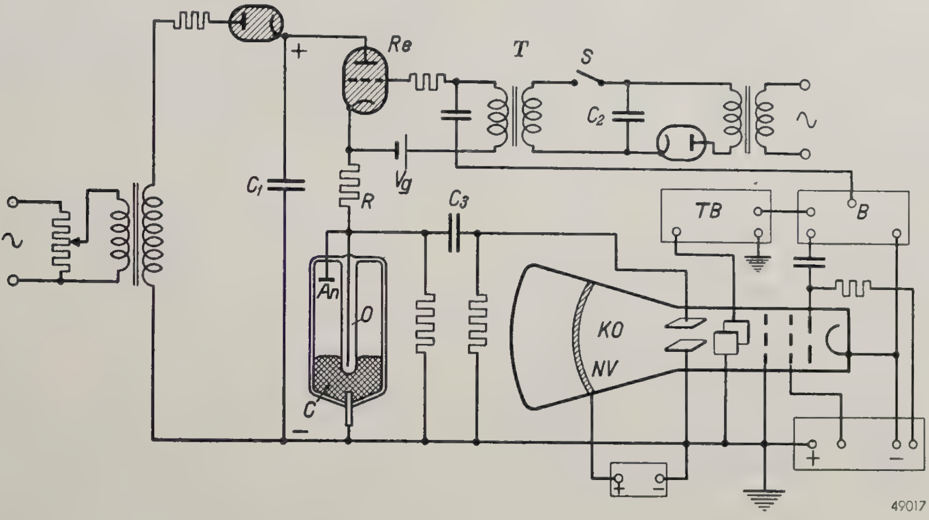

Fig. 6. Circuit for measuring the time lag. The capacitor C_1, charged by a rectifier to a variable voltage, can be discharged across the relay valve *Re*, the resistance *R* and the valve under investigation with the anode *An*, igniter *O* and mercury cathode *C*. The discharge is brought about by depressing the key *S*, whereupon the capacitor C_2 is discharged through the primary coil of the transformer *T*. The voltage impulse thereby excited in the secondary coil causes the relay valve *Re* to ignite, this valve having been previously blocked by the negative grid bias V_g. The variation of the voltage at the starter is observed on the cathode-ray oscillograph *KO*, which is connected with *An via* the capacitive coupling C_3. Since the light spot only describes the oscillogram once, in order to obtain a sufficiently bright image a cathode-ray tube with post-acceleration (*NV*) is employed [7]. In a manner not indicated here, the voltage impulse of *T* at the same time sets in action the generator *B* supplying a voltage of a rectangular form. This voltage releases the electron beam and at the same time causes a calibrated time base (*TB*) to function.

As a check, the time lag of a spark was first measured between two tungsten spheres in a vacuum. With the spheres 0.25 mm apart sparking occurred at 15 kV. The time lag amounted to 2×10^{-7} sec, in agreement with the results of the investigators just mentioned.

In *figs. 7a-d* some oscillograms are reproduced which were obtained from measurements on the discharge tube sketched in fig. 6; the time scale is fixed by fig. 7*e*, the oscillogram of an A.C. voltage with a frequency of 10^6 c/sec. As may be seen, the oscillograms of the voltage on the discharge tube are roughly trapezoidal; in a very short time (here about 5×10^{-8} sec.) — depending mainly upon the capacity of the starter and the resistance of the circuit — the voltage on the starter rises to a value where it remains constant for a certain time, which time we shall consider as the real time lag *T*, after which it falls in 16^{-6}—10^{-7} sec to the arc voltage in mercury vapour at low pressure. The higher the voltage *V* on the starter, the shorter the time *T*. In *fig. 8* *T* is plotted as a function of *V* for four different thicknesses of the starter wall.

The oscillograms show an entirely different picture when the starter is wetted by the mercury, *i.e.* when the mercury meniscus at the starter is

---

[7] A cathode-ray tube with post-acceleration is described in Philips Techn. Rev. 5, 257, 1940.

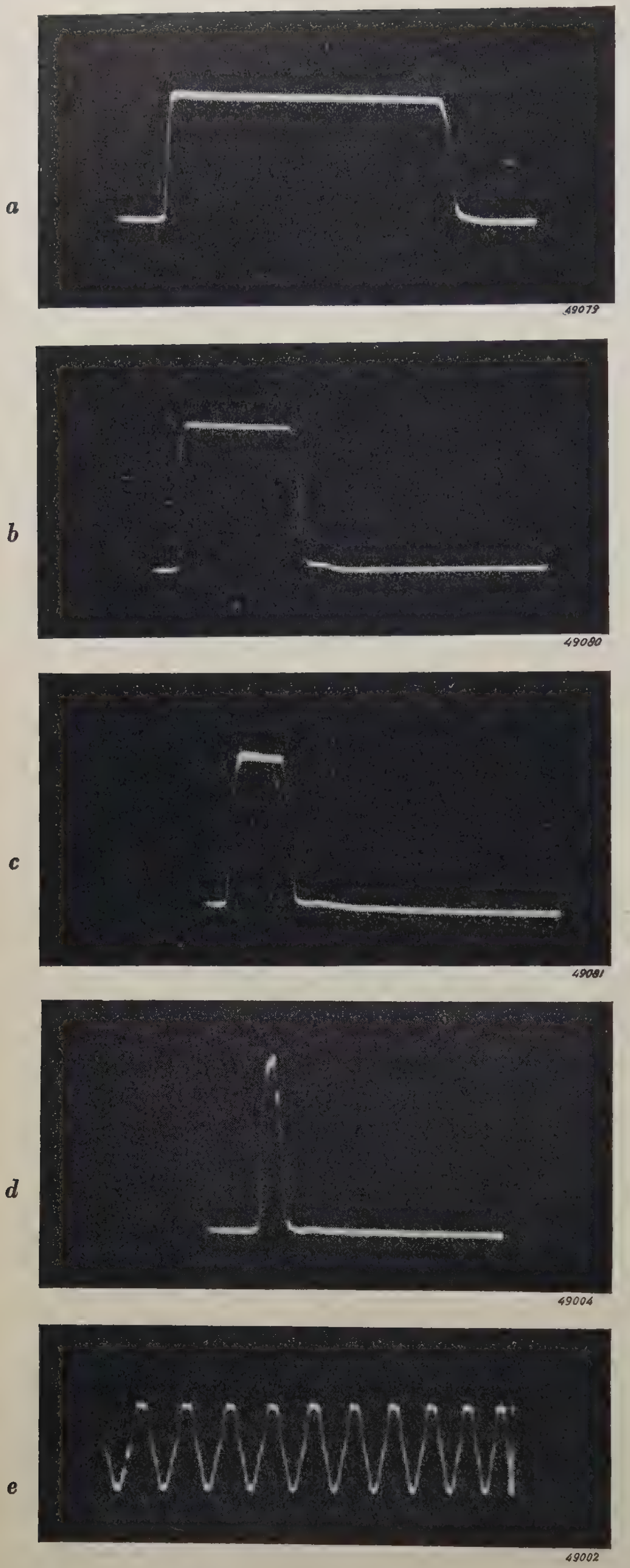

Fig. 7. *a*-*d*) Oscillograms of the voltage between the starter and a mercury cathode with convex meniscus. The voltage V applied to the starter amounted in (*a*) to 5.5 kV, in (*b*) to 6 kV, in (*c*) to 8 kV and in (*d*) to 10 kV. The length of the horizontal part is the real time lag (T). The time scale is given by the oscillogram (*e*) of an A.C. voltage with the frequency 10^6 c/sec. The scale of the ordinates in the figures *a* to *d* is not exactly the same. The oscillograms, like those of fig. 9, were recorded with a cathode-ray tube working with an acceleration voltage of 10 000 V.

not convex but concave, as may happen when there are certain contaminations on the starter wall. Even so, the starter is found to function. *Fig. 9a* shows that even at the low voltage of 1.2 kV there is no real ignition lag (it is to be noted that the time scale here is different from that in fig. 8; it is given by fig. 9*b*, the oscillogram of an A.C. voltage with the frequency 10^7 c/sec.)

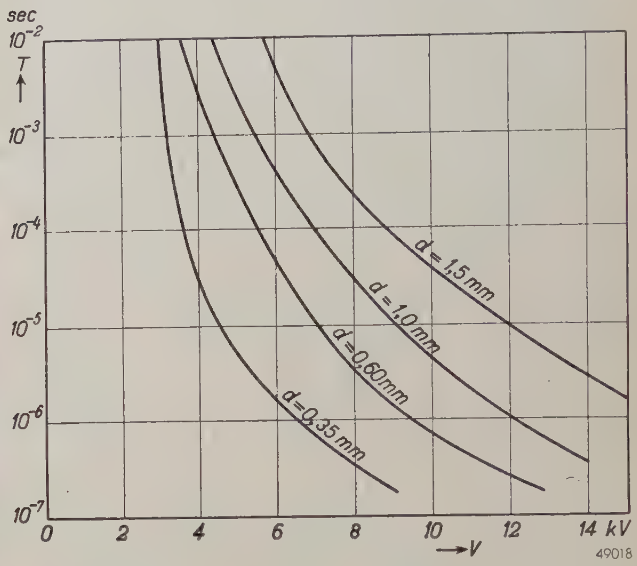

Fig. 8. The oscillographically determined real time lag T as a function of the voltage V applied to the starter; d is the thickness of the wall of the starter.

The microscopic deformation of the mercury surface

We have interrupted the verification of the ignition mechanism described, with the statement that, assuming the surface of the mercury to be smooth, the field strengths found are much too small for any appreciable field emission of electrons. The ignition lag just discussed furnishes the key to the solution of this difficulty. This time lag may be interpreted as the time required for the force exerted by the electric field to cause the formation of the sharp points on the originally macroscopically smooth mercury surface, at which points the field strengths required for field emission are actually reached.

Tonks has calculated the minimum field strength and the time taken to draw out small irregularities on the mercury surface into points [8]); such irregularities are always present owing to the Brownian motion (thermal irregularities). For this minimum field strength Tonks found a value of 53 kV/cm. With higher field strengths the mercury surface becomes unstable, since upon a slight disturbance

---

[8]) Phys. Rev. **48**, 562, 1935.

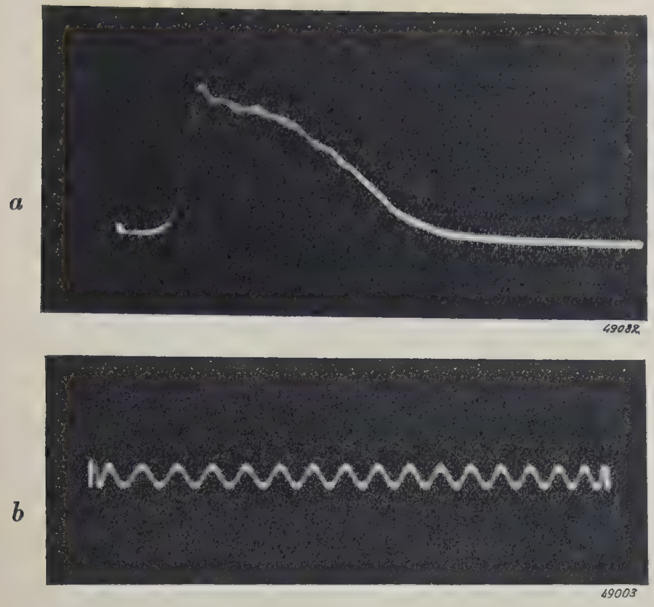

Fig. 9. *a*) Oscillogram of the voltage between starter and mercury cathode with a concave meniscus. There is no time lag here, although the voltage applied is very low, *viz.* 1.2 kV. (N.B. The time base is different from that in fig. 8 *a-d*!)
b) This oscillogram of an A.C. voltage with a frequency of 10^7 c/sec gives the time scale for oscillogram (*a*).

of the equilibrium the drawing force increases more rapidly than the opposing force (capillary force and force of gravity). The time needed depends upon the field strength and the magnitude of the original irregularities. Thus, for example, with a field strength of 2 MV/cm a "hump" 10^{-7} cm in height and with a radius of 10^{-3} cm would be drawn out to a point in 2.3×10^{-6} sec.

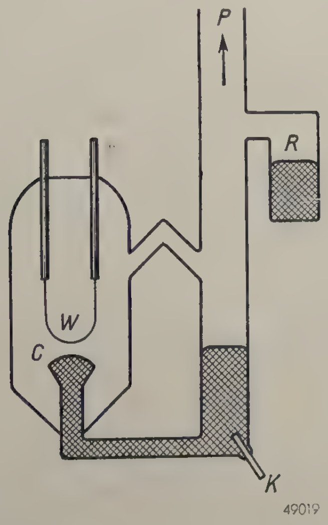

Fig. 10. Experimental tube for measuring the ignition time lag under simplified conditions. The mercury level at *C* is so adjusted (roughly by the addition of mercury from the reservoir *R*, more finely by slightly tipping the tube) as to lie at a distance of 0.25 to 0.125 mm from the tungsten strip *W*. The strip *W* is electrically heated to incandescence before each measurement in order to remove any mercury. *K* current lead, *P* pump tube.

We have investigated these phenomena with a simplified arrangement in which the field strength is directly known and the sparking is brought about in a simpler way due to the absence of the dielectric of a starter. The cathode spot was formed by applying a high positive voltage to an electrode placed at a short distance above the mercury.

In practice this method of ignition is unsuitable, since, in order to obtain the necessary field strength, either very high voltages or a very short distance must be chosen. The latter is quite out of the question owing to the changes in the level of the mercury caused by evaporation or condensation and also the occurrence of waves on the mercury surface caused by mechanical vibrations.

Fig. 10 is a diagram of the experimental tube used. A fine strip of tungsten is mounted at a short distance (0.25—0.125 mm) above the mercury surface; the whole set-up has to be free of vibrations [9]) to avoid any variation in this distance due to ripples on the surface of the mercury.

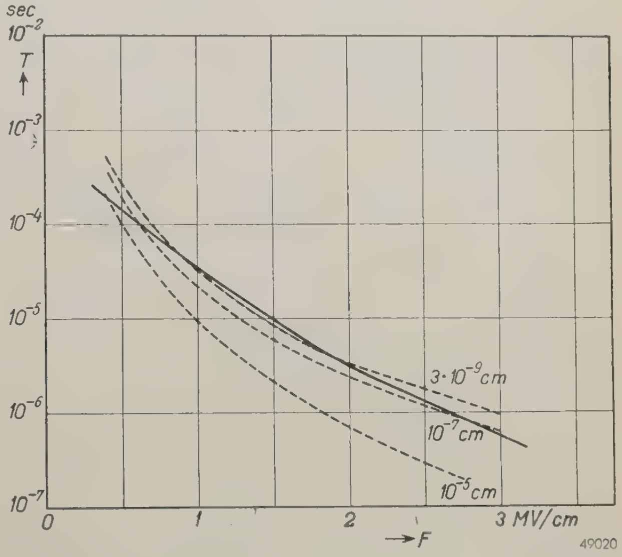

Fig. 11. Continuous line: time lag measured on the tube of fig. 10 as a function of the field strength *F* at the (still smooth) mercury surface.
Dotted lines: times calculated by Tonks for mercury humps to be drawn out into points as a function of *F*, with the height of the humps as parameter. These dotted lines correspond to the continuous line when the height of the humps is about 10^{-8} cm.

The time lags measured according to fig. 7 are represented in *fig. 11* by the continuous line as a function of the field strength *F* at the (still smooth) surface of mercury. The dotted lines in the same graph represent the times taken, according to Tonks, for the mercury "humps" to be drawn out to points; the parameter is the height of the humps.

---

[9]) A very suitable arrangement is for instance that described by J. A. Haringx in Philips Techn. Rev. 9, 16, and 85, 1947 (Nos. 1 and 3).

If we interpret the measured time lags entirely as "drawing-out" times, our measurements agree with Tonks' results when we set the original height of the humps at 10^{-8} cm, the height which Gans also arrived at in his calculation of the irregularity of a mercury surface caused by Brownian motion [10] [11].

This gives a satisfactory explanation of the time lags observed with the tube of fig. 10. In the case of tubes with dielectric ignition, with which we are really concerned, the insulating igniter wall does indeed form a complication, but it is not to be expected that this wall will essentially affect the mechanism on the mercury surface, as will be evident from the following.

Measurements have been carried out with a number of starters with wall thickness d varying from 0.35 to 3.0 mm to determine the field strength F at which time lags T of 5×10^{-3}, 10^{-3}, 10^{-4}, 10^{-5} and 10^{-6} sec. occur. As *fig. 12* shows, the thickness of the wall has very little effect.

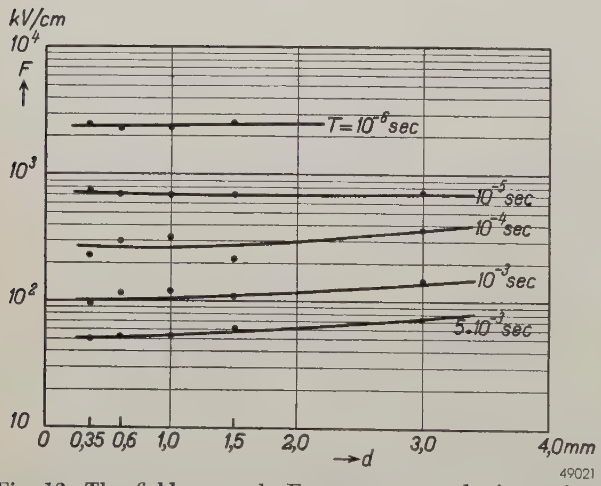

Fig. 12. The field strength F necessary to obtain a given time lag T is found to depend only little on the thickness of wall d of the dielectric igniter.

If for each time lag the average (F_1) of the only slightly varying field strength for the five wall thicknesses is taken and compared with the field strengths F_2 required for the same time lags T in the tube of fig. 10, the two series of results (see *table II*) are found to be of the same order of magnitude.

From this it may be concluded that the field emission on a mercury surface near the wall of a dielectric igniter occurs in the same manner as in the case of an anode electrode placed above the mercury.

Table II. Field strength F_1 in the case of a valve with dielectric igniter compared with the field strength F_2 in the valve of fig. 10, both so chosen that there is the same time lag.

T (sec) =	$5 \cdot 10^{-3}$	10^{-3}	10^{-4}	10^{-5}	10^{-6}
F_1 (kV/cm) =	58	117	286	725	2462
F_2 (kV/cm) =	60	125	625	1500	2700

We must now return for a moment to the measurements of fig. 9*a*, which referred to a concave mercury meniscus. The fact that no time lag was found there is by no means contradictory to what has been stated above. Since the boundary angle α (fig. 2) is acute, it is reasonable to assume that the edge of the mercury is already so sharp as to bring about a field strength sufficiently high for field emission straightaway. Tonks' mechanism of drawing out to points and the accompanying time lag do not then enter the picture.

Summarizing, the course of the process of ignition sketched at the beginning may be defined as follows.

The positive voltage on the starter causes an electric field which, when the meniscus is convex, is not strong enough to bring about field emission on the mercury but strong enough to make that surface unstable. Irregularities due to thermal causes are drawn out to sharp points, for which a certain time is needed (the time lag). At these points the field strength attains values which lead to electron emission. The electron current flows along the starter wall, probably assisted by secondary emission, to an anode. The current concentrated in the mercury points causes Joule heating, as a result of which some mercury vapour is formed which promotes the transition of the discharge into an arc.

Application of relay tubes with dielectric igniter

In the beginning of this article the rectifier was mentioned as an object in which controlled ignition offers certain advantages over other methods. There are, however, many other possibilities of application of relay tubes as switches, for (periodic or non-periodic) current impulses of great intensity and short duration. Such current impulses are required in various fields of technology, for instance for stroboscopic illumination, for spot and seam welding, for transmitters of radar installations, etc. A mercury cathode can safely emit currents of thousands of amperes. In many applications the current impulses are of such short duration compared with the intervals between the impulses that the average value of the current over a length of time

---

[10] Ann. Phys. (Leipzig) **74**, 231, 1924.

[11] A more detailed description of these phenomena will appear in Philips Research Reports.

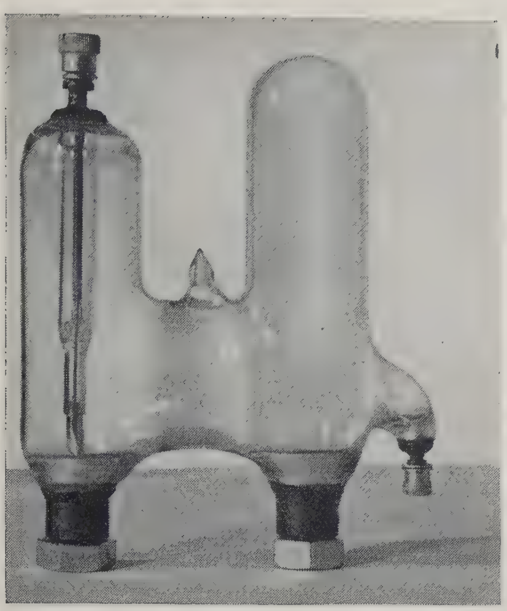

Fig. 13. Relay valve with mercury cathode (left) and dielectric igniter. The anode and the auxiliary anode (right) also consist of mercury in order to avoid contamination of the igniter. The valve, which is about 18 cm in height, can transmit current impulses of 2000 amp. In view of the permissible temperature, the average current is limited to about 1.5 amp. with natural cooling of the valve, and to about 3.5 amp. when a fan is used.

is many times smaller than the impulse current. Since it is the average current, together with the arc voltage, that determines the heat development in the tube, its dimensions can be kept relatively small.

An example of a relay valve for a high peak current but for a much lower average current is shown in *fig. 13*. For this valve, which serves, *inter alia*, as switch in a stroboscope [12]), the peak current is 2000 amp. and the average current only a few amperes. The peculiar shape of the tube is due to the fact that not only the cathode but also the anode and the auxiliary anode consists of mercury. In principle the two latter electrodes could be made of metal or carbon, but then in course of time the surface of the starter would inevitably become contaminated with a film of sputtered anode material, which may lead to irregular ignition. It was therefore made a condition that the inner surface of the tube should consist only of mercury, glass and quartz, so as to ensure that the starter is kept free from contamination.

---

[12]) Described in Philips Techn. Rev. 8, 25, 1946.

DETERMINING THE LIGHT DISTRIBUTION AND LUMINOUS FLUX OF PROJECTORS

by J. BERGMANS and H. A. E. KEITZ.

535.245.24:628.932

In every illuminating engineering laboratory instruments are used for registering the distribution of light from light sources emitting rays in all directions. The light source is suspended in a certain fixed position, the luminous intensity (candle power) is measured in several meridian planes, a polar graph of the light distribution is plotted and from that one calculates the total flux (usually with the aid of a Rousseau diagram). In the case of projectors this method is not directly applicable. If it is a small projector emitting a very narrow beam, the light source can be set up in a fixed position and the light distribution determined by means of a number of isolux curves on a projection screen perpendicular to the optical axis of the beam, the flux then being found by integration. In all other cases the photometer has to be set up in a fixed position and the light beam moved in such a way that each part of the beam is successively thrown on the photometer; for this purpose two different types of rotating apparatus are used. From the results of the measurements taken an iso-candle diagram can be obtained. Before the luminous flux can be determined that diagram has to be reproduced on a flat plane, employing the sinusoidal method or Lambert's azimuthal reproduction, both of which are area-proportional. It has advantages when the measurements are so carried out that the successive directions of measurement lie on a conical surface around the optical axis of the light beam. To make this possible Philips Laboratory for Illuminating Engineering have constructed and are using a special rotating apparatus, which is described in this article.

Introduction

To judge the properties of a light source correctly one should consider not only the total quantity of light emitted but also the manner in which the light is distributed in various directions.

The lamp — the light source proper — is usually mounted in a fitting. In this article we shall use the term light source both for the lamp and for the combination of lamp with its fitting.

Generally one has to do with light sources which emit their light in all directions, or at least within a very wide solid angle. For a long time already appliances have been known and methods have been worked out for determining the light distribution and luminous flux from these light sources.

In this article, however, we are concerned mainly with light sources from which the light flux is emitted in a fairly narrow beam. These are called "projectors". To give an example of such a projector we would recall the fitting with a water-cooled mercury lamp for airfield illumination which has previously been described [1]). That projector produces a flat and fan-shaped beam: vertically the angle of divergence is 2 times approximately 1/2° and horizontally 2 times approx. 40°. Projectors are also widely used for illuminating (floodlighting) facades and suchlike.

We shall explain in this article how in the case of projectors the methods mentioned above need some modification, and we shall describe methods by which it is possible in these cases to register the light distribution and determine the total flux.

Determination of the light distribution and total flux of light sources with multi-lateral radiation

We shall begin by recalling briefly how the light distribution and total flux are usually determined with light sources that radiate in all directions.

The most obvious way is to suspend the light source in a fixed position, preferably in the position in which it is normally used, and then to measure successively the light distribution in a number of vertical planes passing through the light source. In analogy with the usual geographical terminology, these planes are called meridian planes. With the aid of a mirror movable in a meridian plane, or if necessary by means of more than one mirror, the light from the fixed light source is thrown onto a photometer.

Since the introduction of the photocell this is also done by mounting this instrument on a long rotatable arm and turning it in the meridian planes around the light source.

The lux values found in a certain meridian plane can then be plotted in a polar diagram. The light source is taken as lying in the centre and the length of the radius vector indicates what intensity of *I* has been measured in a certain direction. *Fig. 1* gives a specimen of such a diagram.

---

[1]) Th. J. J. A. Manders, Philips Techn. R. 6, 33, 1941.

When the light source is rotation-symmetrical every meridian plane will produce the same polar diagram.

The total flux of a light source is the flux (*i.e.* the quantity of light passing through per second) passing through a spherical surface enveloping the light source. The radius r of that sphere must be chosen in such a dimension that from any point of that spherical surface the light source can be regarded as being situated in the centre of the sphere. If $d\Phi$ is the flux within an infinitesimally small solid angle $d\omega$ bounding a minute area $r^2 d\omega$ of the sphere, then $d\Phi = I d\omega$.

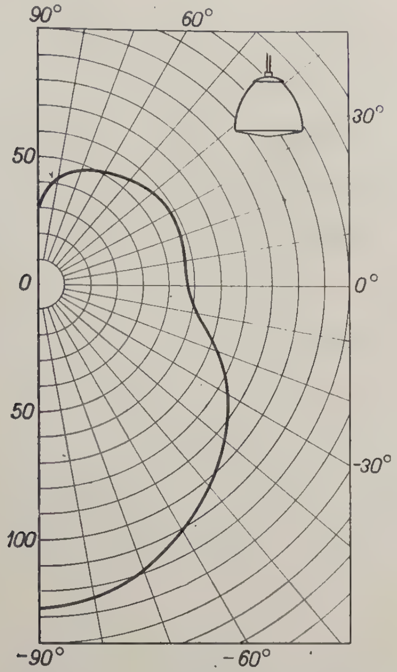

Fig. 1. A polar diagram of the light distribution of a light source in a meridian plane. The radius vector in a certain direction is proportional to the luminous intensity measured in that direction, expressed in candles. The figures given apply for a light source with a flux of 1000 lumens. In agreement with the annotation used in the text, we have taken a horizontal line as the zero direction and set out from that angles up to 90 degrees below and about the zero line. In illuminating engineering one mostly uses a vertical zero line and sets out the angles downward from the top from 0 to 180 degrees. In the top corner is an illustration of the fitting to which this diagram relates.

In the foregoing we have introduced the term meridian planes. We shall now continue to follow the analogy with geographical terms by calling the angular coordinate in a plane perpendicular to the axis, corresponding to the geographical longitude, the longitude l and the coordinate perpendicular thereto, which corresponds to the geographical latitude, the latitude b.

The total flux of a light source is the integral of $I d\omega$, for which we thus find:

$$\Phi = \int_{-\pi/2}^{\pi/2} \cos b \, db \int_{0}^{2\pi} I \, dl \, . \; . \; . \; . \; . \; . \quad (1)$$

In the case of a rotation-symmetrical light source I is independent of l, so that (1) becomes:

$$\Phi = 2\pi \int_{-\pi/2}^{\pi/2} I \cos b \, db \, . \; . \; . \; . \; . \; . \quad (2)$$

This integral is usually calculated by a graphical method, that of the Rousseau diagram. In *fig. 2* it is shown how this diagram is plotted from a polar diagram. A line pq is drawn parallel to the vertical axis of the polar diagram and to the right of it a curve is drawn with $r \sin b$ and I as coordinates. The area contained between this curve, the perpendicular just mentioned and the two drawn horizontal lines pp_1, and qq_1, is proportional to the luminous flux Φ. This area can be determined with a planimeter.

When the beam of light is not rotation-symmetrical the Rousseau diagram cannot be employed in this form, because each meridian plane then produces a different polar curve. If it is, nevertheless, desired to use this diagram for determining the total luminous flux then one must have available candle power measurements found in conical surfaces described about a certain axis selected for the measurement. The average candle power I_b for such a conical surface has then to be determined and substituted for I in formula (2). We shall revert to this later.

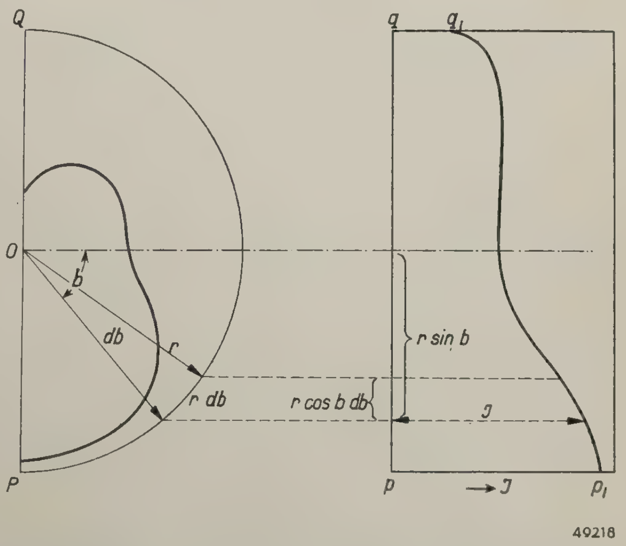

Fig. 2. The calculation of the total luminous flux of a rotation-symmetrical light source with the aid of the Rousseau diagram from the polar graph of the candle power distribution measured in a meridian plane. Here r is the radius of the sphere imagined around the light source, b the latitude in the system of coordinates and I the measured candle power. The area of the figure pp_1q_1q is proportional to the total luminous flux Φ.

Particularly with non-rotation-symmetrical light sources another method is often applied. One then uses an iso-candle diagram. To produce such a diagram one again imagines around the light source a sphere with such a radius that the light source can be regarded as a light-emitting point from any point on the surface of the sphere. One imagines that the candle power of the light source is determined from every point of the sphere and that an iso-candle curve connects the points on the spherical surface from which the same luminous intensity is found. For practical purposes a number of meridian planes can again be measured up with a photometer.

By integration it is possible to derive the total luminous flux from such a diagram by multiplying the area of the strip between two iso-candle curves by the corresponding lux and adding up the result for all strips. But when the planimeter is used to measure the area of a strip one is faced with the difficulty that these iso-candle curves lie on a sphere. It is therefore necessary first to make from that diagram a projection on a flat plane, and this projection has to be "area-proportional". We just mention it here because we shall be reverting to it later on in this article.

We now put the question whether the methods described can be applied to projectors.

Measuring with a stationary projector and a movable photometer

Is it possible to register the light distribution of a projector by fixing this light source and measuring several meridian planes successively with a photometer? Theoretically this is undoubtedly possible. And a polar diagram could then be drawn for each of these planes. But since as a rule in one or more directions the beam is very narrow, in practice it is difficult to apply this method. Think for a moment of the example previously given of a projector where the angle of divergence in the vertical direction is twice approx. 1/2°. But if in one or more meridian planes no reliable polar curve can be drawn then no Rousseau diagram can be employed either, and neither can an iso-candle diagram be constructed. Consequently the methods outlined above are not generally applicable for projectors.

Since projectors emit their luminous flux only in a narrow beam, another measuring method has had to be thought of, where the light source is also set up in a fixed position. By this method a plane is placed perpendicular to the optical axis of the projector (this plane is usually called the projection screen — see *fig. 3*) and the distribution of illumination in this plane is measured and plotted. As the photocell with which this measuring can be done gives the illumination as a direct result, it is logical in this case to record the light distribution from the projector by means of a number of isolux curves (lines of equal illumination) on the projection screen.

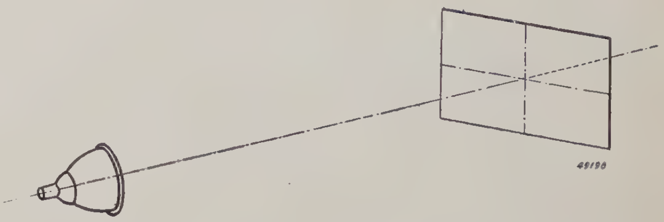

Fig. 3. A projector with a "projection screen" set up perpendicular to the optical axis.

The illumination being equivalent to the luminous flux per unit area, it is easy to determine the flux emitted by the light source. All that is needed is to measure with a planimeter the area between every two isolux lines and multiply by the average illumination of that area.

The method of measuring with a projection screen is applied in practice. It is employed, for instance, with bicycle and motorcar lamps. Sufficiently accurate results can be obtained when the screen is placed at a distance of 6 to 8 metres from the light source.

This method, however, can only be used for small light sources which, moreover, give a beam with a small angle of divergence. The reason is that the luminous body is not a point but has finite dimensions. What is the effect of this upon the beam? A projector consists of a system of reflecting or refracting surfaces, in many cases a rotational paraboloid, as indicated in *fig. 4*. The light source, in this case spherical, is set up in such a way that its centre coincides with the focus of the paraboloid. The part of the light coming from the sphere which strikes the reflector R at the point P_1 is reflected in the form of a conical beam. None of the light from this beam strikes the axis within a certain distance a from the reflector. For a point P_2 on the circumference of the reflector the distance a reaches a maximum value g, the so-called photometrical boundary distance. At points on the axis lying on the projector side of the beam cross-over point the light does not come from the whole reflector but only from its more centrally located parts. When the light distribution of a projector is to be determined the projection screen has to be set up in such a position that the candle power measured there is independent of the distance from the light source. We shall not go farther into the question what the minimum distance between light source and projection screen has to be to achieve this, but suffice it to say that it depends upon the dimensions of the luminous body and the diameter and focal distance of the reflector, and that in any case it must be located beyond the photometrical boundary distance g.

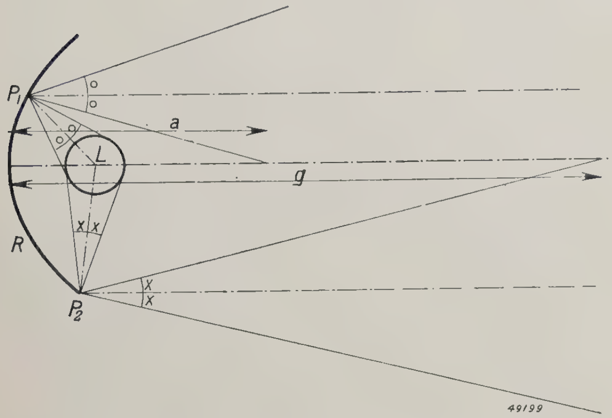

Fig. 4. A spherical light source L with its centre in the focus of the reflecting rotational paraboloid R. None of the light in the beam reflected at P_1 will reach the axis within a distance a from the reflector. For a point P_2 on the edge of the reflector a reaches its maximum value g, called the photometrical boundary distance.

In the case of projectors of a large size (*e.g.* searchlights) the distance of the photometrical boundary distance g to the projector is of the order of several hundreds of metres. It is obvious that even for a beam with a relatively small angle of divergence the measuring method described cannot be applied for such large projectors. The projection screen would be far too large. And this applies, *a fortiori*, when we have to do with a projector having a wide divergence in a certain direction (*e.g.* horizontally).

Measuring with a stationary photometer and a moving projector

In cases where the method with a projection screen cannot be employed another method is followed. The photometer is set up in a fixed position and the projector is turned about a horizontal and a vertical axis, in such a way that every part of the beam is cast in turn upon the photometer. Here again one must take the photometrical boundary distance into account. Consequently in many cases the light distribution from searchlights, such as are used for instance on airfields, cannot be determined in the laboratory on account of the great distance required for measuring it. This must then be carried out in the open field.

From the readings of the photometer an iso-candle diagram can then be constructed as explained in the beginning of this article. These iso-candle curves lie on a spherical surface. As long as the beam divergence does not exceed 5 degrees in all directions around the axis one may safely regard these curves as being lines in a flat plane. By integration one can then determine the luminous flux from that diagram in the manner described above.

If, however, the beam has a wider divergence the results obtained in this way would be too inaccurate. In such a case, before using the planimeter, one has to make a projection of the iso-candle diagram on a flat plane by one of the methods to be discussed below.

In literature there are two types of rotating apparatus described. It may be so constructed that the horizontal axis of rotation is a shaft contained in bearings in the fixed frame. The apparatus then turns first around this fixed horizontal axis and then also around an axis starting in the vertical position and following the rotation about the horizontal axis (*fig. 5*). It is also possible, however, to have the vertical shaft in fixed bearings and the horizontal axis following the movement around the vertical axis (*fig. 6*); this is the second type of apparatus. Both types of apparatus are used in laboratories for illuminating engineering. There is no international agreement as to which type is to be taken as standard. This is to be regretted, because when an iso-candle diagram is given in literature one is at a loss to know with what type of apparatus the light distribution was measured, unless it is

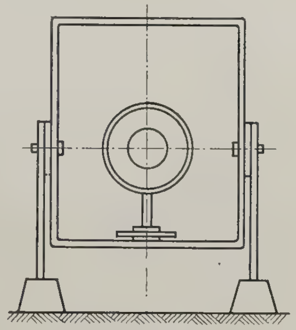

Fig. 5

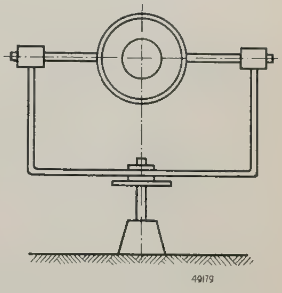

Fig. 6

Fig. 5. A measuring apparatus where the projector turns about a fixed horizontal axis and also about an axis which in the position of rest is vertical and upon rotation follows the movement of the horizontal axis.
Fig. 6. A measuring apparatus where the light source turns about a fixed vertical axis and also about a horizontal axis following the movement of the vertical axis.

specifically quoted, and as a consequence in some cases, as will appear farther on, the results given may be misconstrued.

To ascertain what difference it makes in the shape of an iso-candle diagram whether an apparatus is used of one type or of the other, we must bear in mind that what we want to construct is a diagram showing the candle power of a projector emitted at a certain angle to its axis. In the construction of the diagram we therefore imagine the projector as fixed and plot the angle deviations at which the measurements have been taken. When the actual measurements are being taken, however, it is in fact the photometer that is fixed and the projector is rotated. When, therefore, the projector is turned "to the right upward" the direction of measurement with respect to the axis of the beam has a deviation "to the left downward". And then we must first consider how the diagram just referred to can be constructed in a flat plane.

Projecting the spherical figures onto a flat plane

The manner in which an iso-candle diagram as determined on a spherical surface can best be projected onto a flat plane is not a new problem in illuminating engineering. It is in essence the same problem with which any geographer is faced when producing a map. Euler has already proved that it is not possible to project spherical figures onto a flat plane so as to give a true reproduction both of the shape and of the area of the figures. There are, however, several methods in use by which a projection is obtained that gives either one or the other feature of the figure in its true dimensions.

The sinusoidal projection

A familiar method in geography is the so-called sinusoidal projection. When we take a point on a sphere (with radius r) and indicate that with the coordinates longitude l and latitude b, then by this method that point is determined on the flat plane by the flat coordinates:

$$x = rl \cos b, \qquad y = rb.$$

This sinusoidal projection is widely used in photometry because it has the advantage of being area-proportional.

We shall use this sinusoidal projection method to compare the iso-candle diagrams obtained from observations and with the apparatus illustrated in figs. 5 and 6.

With the apparatus of fig. 5 we have to do with a system of spherical coordinates, where we may regard the angle of rotation around the horizontal axis as longitude and the rotation around the other axis as a movement in latitude. The poles of this system lie in the horizon in a direction perpendicular to the optical axis of the projector and the equator passes through the zenith. As the apparatus turns about the vertical axis the measuring direction describes meridians, and as it turns about the horizontal axis it describes circles of latitude. In *fig. 7* we see how these meridians and circles of latitude are represented in a sinusoidal projection.

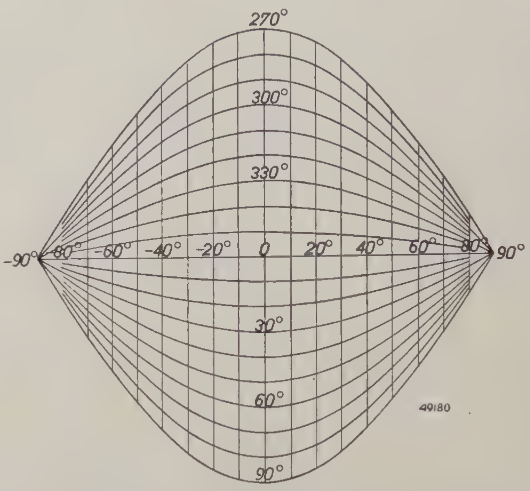

Fig. 7. The sinusoidal projection of the grid belonging to the measuring apparatus of fig. 5.

With the apparatus of fig. 6 we have to regard the rotation around the fixed vertical axis as a movement in longitude and the angle of rotation around the other axis as latitude. The poles coincide with the zenith and the nadir, and the equator coincides with the horizon. As the apparatus turns around the horizontal axis the measuring direction describes meridians and as it turns around the vertical axis

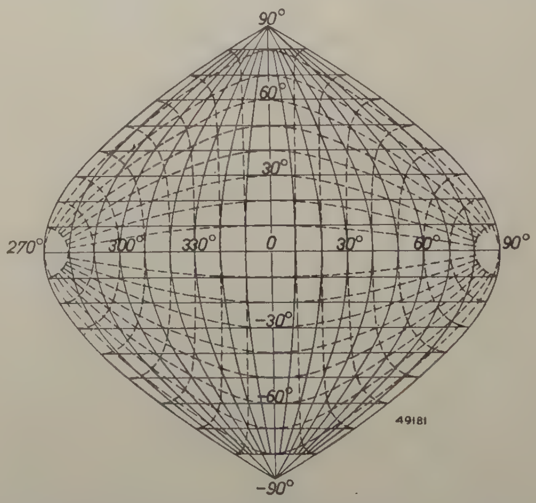

Fig. 8. For comparison some meridians and small circles of fig. 7 are shown as dotted lines on the sinusoidal projection of the grid belonging to the measuring apparatus of fig. 6.

it describes circles of latitude. In *fig. 8* we have the grids corresponding to the movements in this system projected sinusoidally, whilst for comparison some of the meridians and circles of latitude from fig. 7 are interposed in dotted lines.

When the angle of divergence of the beam is small, it will not make much difference as regards the calculated luminous flux whether or not we know which rotating apparatus has been employed in determining the light distribution. But when we have to do with a divergence angle of say 20 degrees it would be an intolerable mistake to interpret measurements taken with an apparatus of fig. 5 as having been taken with such an apparatus as illustrated in fig. 6.

To give an idea of what this mistake would mean we have reproduced in *fig. 9* on a magnified scale the middle part of the diagram of fig. 8. It is seen that the bearing, for instance, indicated with the apparatus of fig. 6 as lying 30 degrees north and 30 degrees west (point *A* in fig. 9) makes an angle of approximately 5 degrees with the position obtained from the same bearings indicated with the apparatus of fig. 5 (point *B* in fig. 9). Obviously, then, when measuring beams with a wide divergence it is essential always to state with what type of apparatus the measurements have been taken.

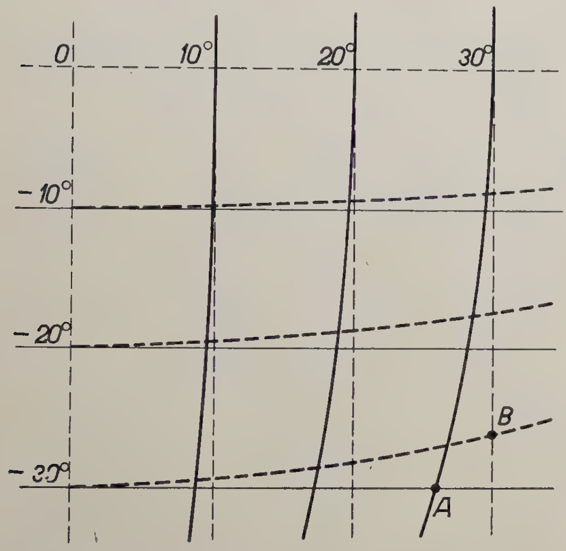

Fig. 9. The middle part of the diagram illustrated in fig. 8 on a magnified scale. The bearing indicated by 30° north and 30° west (point *A*) by means of the apparatus according to fig. 6 makes an angle of about 5 degrees with the same bearings obtained with the apparatus of fig. 5 (point *B*).

Fig. 10 is a sinusoidal projection of an iso-candle diagram of a light source emitting its light in a rather narrow beam. As already indicated, the total luminous flux from this light source can be calculated by measuring with a planimeter the area between two iso-candle curves at a time and multiplying it with the estimated average candle power of that area.

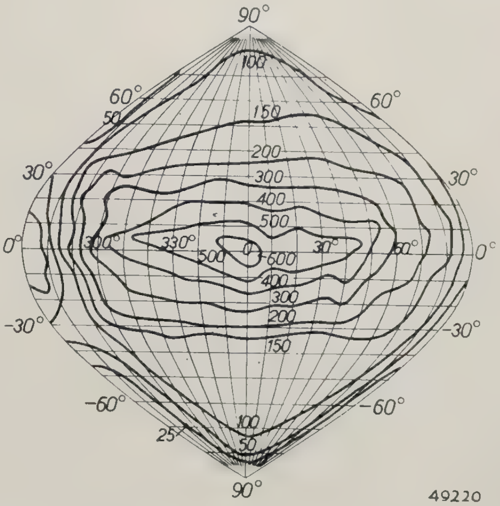

Fig. 10. The iso-candle diagram of a "Cornalux" lamp in sinusoidal projection. The luminous intensity is given in candles, whilst the total luminous flux of this light source amounts to 1320 lumens. From the diagram it may be read that this lamp, which is used for ceiling lighting, emits its light in a rather narrow beam.

The azimuthal projection

If it is desired to represent in a flat plane a figure lying on a sphere one does not necessarily have to use the method of sinusoidal projection. Another method, which is not only employed in geographical work but can also be applied in photometry, is the azimuthal projection according to Lambert. This, too, is area-proportional.

With this method of projection the area of a hemisphere is projected with a circle. The meridians

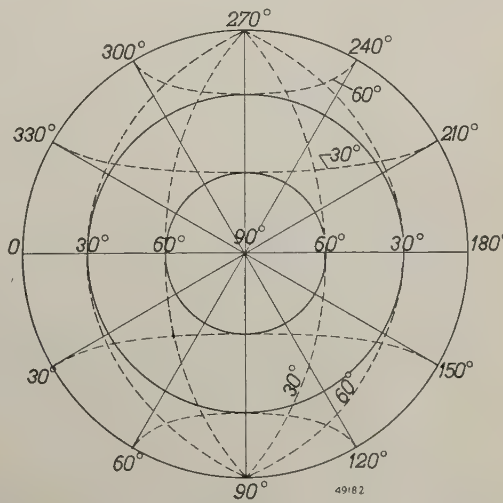

Fig. 11. The azimuthal projection of a spherical grid according to Lambert. The full lines represent some meridians and circles of latitude of a system of coordinates whose polar axis is perpendicular to the drawing plane. The dotted lines are some meridians and circles of latitude of the system of coordinates corresponding to the rotating apparatus of fig. 6.

are drawn as one sees them when looking at a sphere in the direction of the polar axis, thus as diameters of the edge circle or the equator. The lines of latitude are represented by circles concentrical with the edge circle.

In discussing the systems of spherical coordinates as applying to the apparatus of fig. 5 the polar axis is a horizontal line perpendicular to the optical axis of the projector and in the case of fig. 6 a vertical line likewise perpendicular to that optical axis.

There is, however, a third system of coordinates that can be used, where the polar axis is coincident with the optical axis of the projector in its zero position. We shall now first consider this system of coordinates. It is illustrated in *fig. 11*. There we see some meridians drawn (diameters of the outer circle) and some circles of latitude. When we represent in this system of spherical coordinates the longitude as l' and the latitude as b', and the radius of the sphere as r, we find for the coordinates of the plane figure:

$$x = 2\,r \sin\,(45° - 1/2b')\cos l'$$

and

$$y = 2\,r \sin\,(45° - 1/2b')\sin l'.$$

One can draw in the same figure also the spherical grids appertaining to the two other systems of coordinates mentioned above. In fig. 11 we have indicated in dotted lines some meridians and circles of latitude of the spherical system belonging to the apparatus of fig. 6. The poles of this system, as explained before, coincide with the zenith and the nadir. When we represent the longitude and latitude of this system as l and b, as before, then for the coordinates of the plane figure we find:

$$x = r\sqrt{2}\,\frac{\sin l \cos b}{\sqrt{1 + \cos l \cos b}}$$

$$\text{and } y = r\sqrt{2}\,\frac{\sin b}{\sqrt{1 + \cos l \cos b}}.$$

In the Lambert projection we may now — just as by the sinusoidal method — indicate the measured candle power in the directions of the points of intersection of the meridians and circles of latitude every 5 or 10 degrees and from that derive the iso-candle curves by interpolation. To arrive at the luminous flux the area of each segment between two iso-candle curves is again measured with the planimeter and the result multiplied by the corresponding average candle power. For this we need a new interpolation. The result, therefore, is not always sufficiently accurate, especially where the light distribution is most irregular.

In *fig. 12* we see the light distribution of the Philips fitting ZE 30 [2]) as used for road-lighting represented in *a*) a sinusoidal projection and *b*) an azimuthal projection.

A comparison of these two shows that the latter has some advantages. In the Lambert projection there is little distortion of the figures; a small circle on the sphere is projected as a circle round about the centre and as an ellipse close to the edge, with the axes in a ratio of 2 : 1. This is due to the fact that the scale on which one degree in a radial

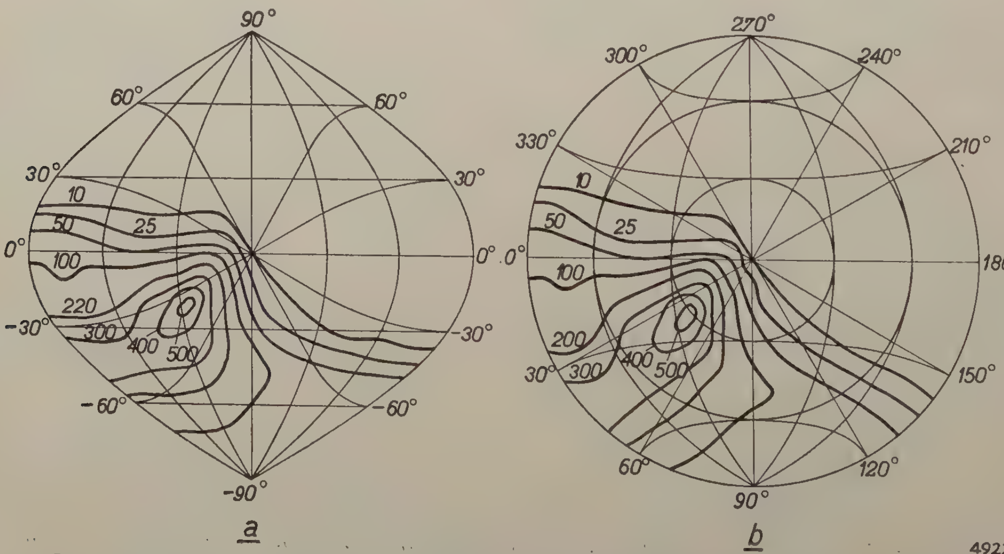

Fig. 12. The iso-candle diagram of a light source for road lighting (fitting Philips ZE 30) in *a*) sinusoidal projection and *b*) azimuthal projection according to Lambert. The other hemisphere is symmetrical with the one represented here. The luminous intensity is given in candles for a light source with total luminous flux of 1000 lumens.

---

[2]) See Philips Techn. R. 5, 231, 1940.

direction has to be plotted differs but very little for the various parts of the diagram. Within the circle of a radius of 30 degrees about the axis (thus between $b' = 60^\circ$ and $b' = 90^\circ$) this scale is even practically constant. It is likewise an important advantage that this greatly facilitates interpolation in the diagram. It is true that in the Lambert projection the meridians and circles of latitude of the network belonging to the apparatus of fig. 6 do not as a rule intersect exactly perpendicular to each other, but the deviations from 90° are not so great as is the case with the sinusoidal projection. Furthermore, with the latter projection one cannot see whether a beam is rotation-symmetrical, as is in fact possible with the Lambert projection.

Upon studying the shape of projection of the network in fig. 11 we notice that all bearings lying on one conical surface, having as its axis the optical axis of the projector, are represented in the diagrams as points on one circle (concentrical with the edge circle). This leads us to put the question whether it would not be desirable to arrange the measuring in such a way that the successive bearings lie on a conical surface around the optical axis. This requires a rotating apparatus making it possible to obtain these results quickly and concisely. Such an apparatus we shall now discuss.

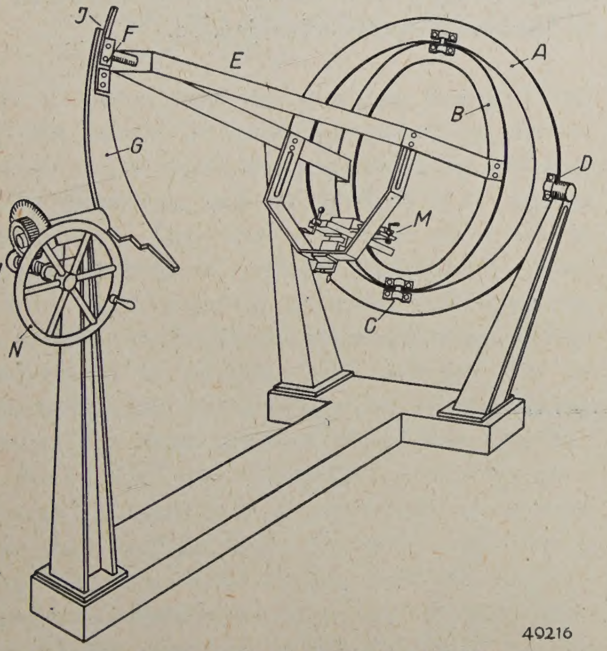

Fig. 13. Diagrammatic representation of the rotating apparatus described for projectors. The projector is suspended on the principle of a cardan joint by fixing it inside the inner one of two rings *A* and *B* rotatable about the gudgeons *C* and *D*. Attached to the inner ring is a fork *E*. By means of a sliding joint *F* this fork can be moved and fixed on a graduated segment *G* that can be turned about its other end by means of a worm gear *H*. The sliding joint and the fork are connected by a ball fitting exactly in a cylindrical hole in the sliding joint. By means of a vernier *J* adjustments can be made accurately to within one-eighth degree. Further the fork *E* is fitted with a bracket to which an adjusting device *M* is attached, consisting of turning-lathe supports and making it possible to adjust the projector accurately.

The Philips rotating apparatus for measuring projectors

In Philips laboratory for illuminating engineering an apparatus has been constructed which makes it possible to carry out measurements in a simple way in conical planes around the axis. This will be described with the aid of the illustration in *fig. 13*; two photographs of the apparatus are reproduced in *figs. 14* and *15*.

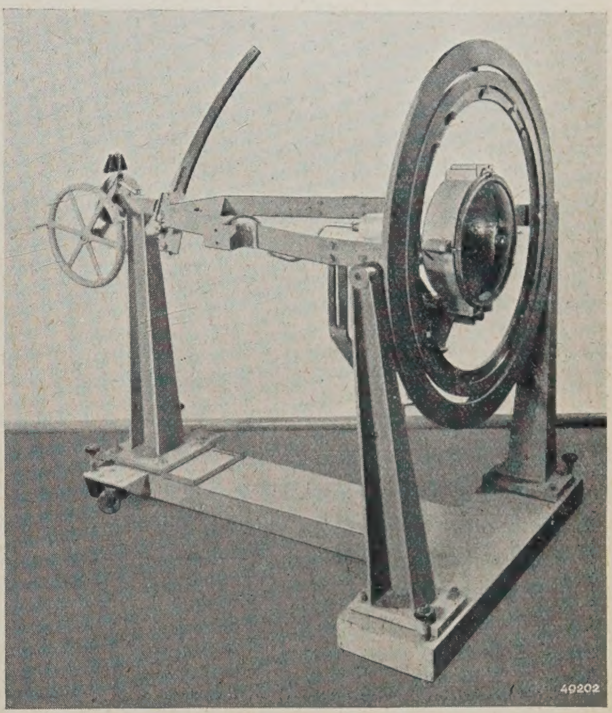

Fig. 14. The Philips measuring apparatus, with a "Philiflood" floodlight mounted in it.

The projector is suspended by an arrangement on the principles of a cardan joint, by fixing it inside the inner one of two rings rotatable about two pairs of gudgeons. Attached to the inner ring is a fork *E*. By means of a sliding joint *F* this fork can be moved and fixed on a strong graduated arc made rotatable at the other end by means of a worm gear. The sliding joint *F* is connected with the fork by a ball fitting exactly into a cylindrical hole in the sliding joint. A vernier allows of adjustments accurate to one-eighth degree. Further, on the fork *E* is a bracket to which an adjusting device is attached consisting of turning-lathe supports and making it possible to adjust the position of the projector accurately.

By adjusting the sliding joint *F* to a certain number of degrees on the graduated arc and turn-

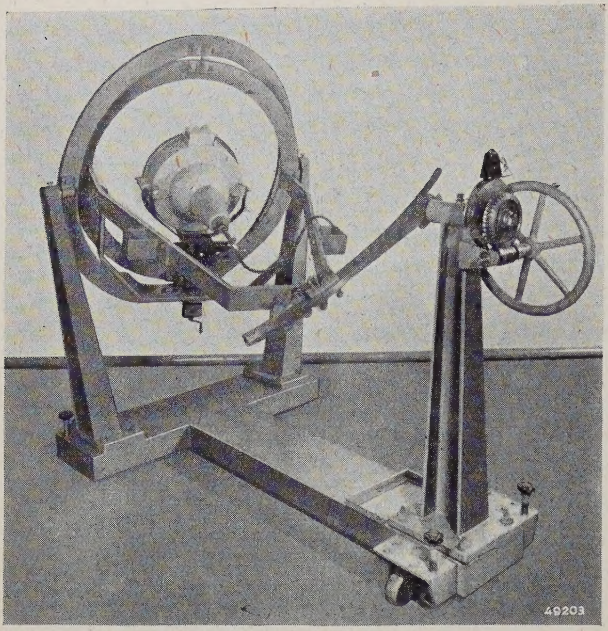

Fig. 15. The rotating apparatus when registering the light distribution of the floodlight in a different position.

ing this arc by means of a handwheel and the worm gear, a large number of measurements can be taken which all give the candle power values in directions making the same angle with the axis of the light source.

This rotating apparatus offers advantage first and foremost when applying the azimuthal method of projection. We have already remarked that in this form of projection all bearings lying on the same conical plane are represented in the diagram as points on a circle. Further, all bearings measured while the segment G is in the same position will be represented in this diagram (fig. 11) by points lying on the same radius from the origin (O).

In the second place it is advisable to use this instrument when the luminous flux of projectors is to be determined with the aid of the Rousseau diagram. The arithmetical mean then has to be determined of all measurements relating to the same angle of deviation from the axis. In this way it is possible to find accurately the average candle power from the projector in a given conical plane. This is then plotted in the Rousseau diagram in the manner explained in the beginning of this article.

The rotating apparatus described above therefore makes it possible, with the help of the Rousseau diagram, to determine the luminous flux of a projector more quickly and more accurately than would be possible with one of the apparatuses of fig. 5 and fig. 6 when employing the sinusoidal or the azimuthal method of projection.

ABSTRACTS OF RECENT SCIENTIFIC PUBLICATIONS OF THE N.V. PHILIPS' GLOEILAMPENFABRIEKEN

Reprints of the majority of these papers can be obtained on application to the Administration of the Research Laboratory, Kastanjelaan, Eindhoven, Netherlands. Those papers of which no reprints are available in sufficient number, are marked with an asterisk.

1712: E. J. W. Verwey (+ J. E. Asscher): Lattice structure of the free surface of alkali-halide crystals (Receuil Trav. Chim. Pays-Bas **65**, 521-528, 1946).

Calculations have been made of the lattice distortion at the free crystal surface of the cube face of alkali halide crystals on the basis of Born's lattice theory, with the result that the displacement of the positive surface ions in a direction perpendicular to the surface differs considerably from that of the negative. A kind of ionic double layer is formed with the negative ion pointing away from the crystal. The corresponding dipole is more or less compensated by the dipole moment induced in the negative ions. This distortion lowers the surface energy as is illustrated by the calculation for the case of NaBr.

1713: J. Th. G. Overbeek and P. W. O. Wijga: On electro-osmosis and streaming potentials in diaphragms (Rec. Trav. Chim. Pays-Bas **65**, 556-563, 1946).

It is stated that the streaming potential E/P and the volume of liquid transported by electro-osmosis v/i are equal, independent of the structure of the diaphragm and independent of its surface conductance. The value of these ratios which, in the absence of surface conductance, equal $\varepsilon\zeta/4\pi\eta\lambda$ (ε = dielectric constant, η = viscosity, λ = electric conductivity) diminishes when surface conductance is present. This decrease can be accurately taken into account when the diaphragm consists of a single capillary of constant diameter. In the case of real diaphragms, consisting of a network of capillaries of different shape and dimensions the correction factor for surface conductance cannot be computed! It has been the common practice to estimate the correction factor from the ratio of the observed to the calculated electric resistance of the diaphragm. This procedure is shown to be erroneous, leading to values of the *ö*-potential that are essentially too low.

1714: J. M. Stevels: The physical properties of glass in relation to its structure (J. Soc. Glass Technology **30**, 31-53, 1946).

A fairly extensive account is given of the knowledge we have at present of the structure of glass in general. On this basis some physical properties of glass *viz.* the density and the electric conductivity, are discussed in detail. The density of „normal" glasses can be calculated satisfactorily by means of a formula containing only two constants. One of these constants gives valuable information about the structure of the glass, especially about the way in which the „excess" of oxygen is taken up by the network. The electric conductivity-temperature relationship is briefiy discussed.

1715: J. A. Haringx: The Notch-Impact Test according to Schnadt („De Ingenieur" **58**, Mk 15-17, 1946).

A new type of notch-impact bar has been introduced by Schnadt. With this bar the bending pressure does not act upon the material itself but on a hardened steel pin. Since the centre line of this pin functions more or less as the axis of rotation and the material itself is thus entirely subjected to a tensile load, this is really a sort of impact-tensile test. The greatest advantage lies in the fact that every test bar breaks, even if no other notch is made in it. This makes it possible, with the same cross section of fracture (3 × 10 mm^2), to make several notches with greatly different radius of curvature. Consequently a series of widely divergent stress conditions can be created.

1716*: H. A. Klasens: The light output of zinc sulphide on irradiation with alpha rays (Trans. Faraday Soc. **42**, 666-668, 1946).

A critical review of the literature dealing with the light output of ZnS excited with alpha rays shows that, in most measurements values are found of 10—15% and of the same order of magnitude as those found with cathode rays, in accordance with the theories of Thomson, Bethe and others.

The author refutes the much higher value (80%) given by Riehl without giving accurate data about his measure monte.

1717: J. M. Stevels: The physical properties of glasses.

III. The density of borate glasses

IV. The density of phosphate and germanate glasses.

(J. Soc. Glass Techn. **30**, 173-197, 1946).

The theory given is an earlier communication *), on the density of silicate glasses (as a fuction of their composition) is extended to borate, borosilicate and boro-aluminate glasses. It is shown that in these three cases there is an "accumulation region" (where the O ions form tetrahedral instead of triangular configurations round the B^{3+} ions) and a „destruction region" (where the O^{--} ions are taken up by the breaking of linkages between the network formers). For the boro-aluminates a „crystalline region" (where at least two phases are formed, of which at least one is crystalline) occurs as well. Methods are given for calculating the density. The values so derived are in satisfactory agreement with those obtained by experiment. The theory given is found to hold also for phsophate and germanate glasses.

---

*) J. M. Stevels, Rec. trav. chim. Pays Bas **60**, 85, 1941; **62**, 19, 1942.

Number 2 of Volume 2 (April, 1947) of *Philips Research Reports* contains the following papers:

R 37: J. L. Meyering and M. J. Druyvesteyn: Hardening of metals by internal oxidation; part I

R 38: H. C. Hamaker: Radiation and heat conduction in light-scattering material, II General equations including heat conduction.

R 39: H. C. Hamaker: Radiation and heat conduction in light-scattering material, III Application of the theory.

R 40: A. van Weel: An improved method of coupling valves at ultrashort waves.

R 41: F. L. H. M. Stumpers: Interference problems in frequency modulation.

Readers interested in any of the above mentioned articles may apply to the Administration of the Philips Physical Laboratory, Kastanjelaan, Eindhoven, Holland, where a limited number of copies are available for distribution.

For a subscription to Philips Research Reports please write to the publishers of Philips Technical Review.